OPTIMUM RESOLUTION IN NUMERICAL WEATHER PREDICTION

By

ATUL KUMAR VERMA

DEPARTMENT OF MECHANICAL ENGINEERING

INDIAN INSTITUTE OF TECHNOLOGY KANPUR

AUGUST 1992

OPTIMUM RESOLUTION IN NUMERICAL WEATHER PREDICTION

A Thesis Submitted

in Partial Fulfilment of the Requirements

for the Degree of

MASTER OF TECHNOLOGY

By

ATUL KUMAR VERMA

to the

DEPARTMENT OF MECHANICAL ENGINEERING

INDIAN INSTITUTE OF TECHNOLOGY KANPUR

AUGUST, 1992

CONTENTS

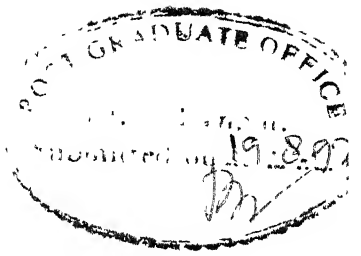

CERTIFICATE

This is to certify that the work entitled 'Optimum resolution in Numerical Weather Prediction' by *Atul Kumar Verma* (Roll NO. 9010511) has been carried out under my supervision and that no part of this work has been submitted elsewhere for any degree.

August, 1992

(Dr. Vinayak Eswaran)
Asst. Professor
Department of Mechanical Engineeri
Indian Institute of Technology, Kan
Kanpur - 208016, INDIA

ACKNOWLEDGEMENT

With a profound sense of gratitude I express my sincere thanks to my Gurudev and guide Dr. Vinayak Eswaran for his invaluable guidance throughout the course of this work. Only because of his patient guidance and encouragement, I have been able to complete this work. He is always a source of inspiration to me. I humbly express my indebtedness for all that he has done for me during my illness and stay here.

I wish to express my gratitude to my friends Ajay, Amren, Dharmendra, Geetu, Mahendra, M. V. Rao, Pramod, Rajeev, Rajesh, Ravindra, Ruta, Shamsi, Shinu, Siva, S. Srinivaslu, Subhash Mishra and Ved prakash for making my stay here, a memorable one.

Atul Kumar Verma.

LIST OF FIGURES

LIST OF TABLES

NOMENCLATURE

a	Radius of the earth
f	Coriolis parameter ($=2\ \Omega \sin\phi$)
$\hat{i}, \hat{j}, \hat{k}$	Unit vectors
k	Verical wave number; index
m	index
n	index
p	pressure
r	Radial distance; Root mean ssquare (RMS)
$\hat{r}$	Radius vector
t	Time coordinate
u	x-component of velocity
v	y-component of velocity
w	z-component of velocity; Weight-function
x,y,z	Space coordinates
D	Depth scale
Fr	Friction force
H	Scalar field
J	Jacobian
L	Wave length; Horizontal Length Scale
N	Rhomboidal Truncation wave number; index
P_n^m	Associated Legendre Polynomial
T	Time scale
$\hat{U}$	Velocity relative to the earth
$\hat{U}_a$	Absolute velocity
$\hat{V}$	Horizontal velocity
U	x-component of velocity $\times \cos\phi$

V	y-component of velocity $\times \cos\phi$
Y_n^m	Spherical Harmonic
β	Rossby parameter(=df/dy)
δ	Kronecker delta
∇	Del operator
ζ	Vertical component of Vorticity
λ	Longitude
μ	$=\cos\phi$
ρ	Density; random number
σ	Standard deviation
ψ	Stream function
ϕ	Latitude
Ω	Angular velocity of earth

ABSTRACT

The initial conditions (IC) used in Numerical Weather Prediction (NWP) codes have a degree of uncertainty, due to observational and other errors. Given this, it is futile and computationally expensive to increase the resolution of these numerical simulations beyond the point where the resolution errors becomes secondary to initial condition dependent (ICD) errors. In an attempt to find an optimum resolution, in terms of a spectral truncation number N, the resolution and ICD errors in a Spectral Barotropic Vorticity model is studied. A case is made as to why the study of this simple model yields the upper limit of the resolution required by more realistic models. It is found that, given error in the IC of 5-10% RMS(root mean square), N=32 produces more than adequate resolution for three day predictions of the velocity field. The vorticity field, however, requires higher resolution. It is found that the the errors induced by truncation of IC grows quite slowly with time. Another interesting observation is that, for the same overall RMS error, the predictions are much more sensitive to errors in the lower order spectral coefficients than in the higher order ones in the initial conditions.

CHAPTER ONE

INTRODUCTION

Historical Background :

The cornerstone of the scientific weather forecast is th so-called *synoptic* (same-time) map of the current conditions (i.e pressure, velocity etc.) over an area spanning distances of th order of a thousand kilometers (called the *synoptic scale*) in eac direction. These maps can then be used to predict the weather fo the following few days, by the use of either the forecaster's skil which combines experience, scientific reasoning and well-developed intuition, or by the use of numerical models.

However, the first synoptic map of surface pressure was no constructed until 1820 and then only with data nearly 50 years old It was only after the invention of the Telegraph in 1845 tha synoptic maps could be constructed fast enough to be used i operational forecasting. During the period called the *empirical er* (1850-1920), weather organizations to provide forecasts for th general public, agriculture, flood warning, transportation, etc were founded. But the forecasting in this period relied solely o the skill of forecasters in interpreting synoptic charts and othe observed data.

Bjerknes, in 1904, realized that the motion of the atmospher is fundamentally a solution of the basic equations of fluic mechanics. Bjerknes also realized that this system of non-linear

partial differential equations did not posses a general solution, and that, in addition, the data-gathering capability in his time was wholly inadequate to determine the initial conditions for the initial value problem involving the fluid flow equations.

Less than two decades later, L. F. Richardson attempted to solve the system of equations numerically using manual calculations (which involved *months* of tedious work). This pioneering effort, published in 1922, unfortunately predicted pressure changes of an order of magnitude greater than actually observed. It is now known that Richardson had made a fundamental error in his approach - the numerical time-stepping scheme used was *unstable* (fundamental work on numerical instability was done by Courant, Friedrichs and Lewy a few years *after* Richardson had published his work). But the result of the first numerical simulation of the atmosphere was to discourage other similar attempts for three decades till the invention of the first practical electronic computers. However, the invention of the radiosonde, during this period, led to further empirical improvements in forecasting. Meanwhile, theoretical research laid the foundation for a departure from pure empiricism.

Electronic computers provided the last ingredient needed for a breakthrough. In 1950, Charney, Fjørtoff, and Von Neumann produced the first successful numerical forecast using an equivalent-barotropic vorticity model which was far simpler than the one developed bv Richardson. The weather predictions made with this simple model, however, were nearly as good as those made by highly skilled forecasters using empirical techniques. With this success, numerical weather prediction (NWP) was soon on the way to becoming the primary tool for modern weather forecasting.

During the last four decades there have been rapid advances in all aspects of NWP, supported by almost incredible developments in the speed and memory size of electronic computers. The development of meteorological satellites has provided global observations that have spurred new insights about the weather. Satellites have also been very valuable for short-range disaster warnings of hurricanes etc., especially over and near areas with few other observational platforms. However, data-gathering from these satellites has not yet reached the sophistication and accuracy needed in providing initial conditions for NWP.

Numerical weather forecasting requires a closed set of governing equations (which are generally partial differential equations), suitable initial and boundary conditions, and a numerical method for solving the initial boundary value problem implied in forecasting. The boundary conditions provided in a global model will be the natural periodic boundary conditions. However, if NWP is being attempted using a limited area model, some artificial boundary conditions are devised so as to be able to solve the problem.

Obtaining the initial conditions for the numerical prediction codes is not a trivial task. It involves the collection and checking of surface- and upper-air meteorological observations, which work forms the bread-and-butter activity of most meteorological stations. However, this data cannot be directly used as initial conditions because, firstly, the initial conditions are to be specified over a given set of grid points covering the forecast region, which generally will not coincide with the positions of the observation stations. Therefore, some form of interpolation has to be used. Furthermore, the raw or interpolated

data, due to observational or interpolation errors, may contain energy in certain scales (length or time) which cause the initial data to be unphysical or which may cause the computations to become unstable. Therefore the raw data is subjected to dynamical and statistical constraints, which are used to 'massage' the data into a form in which the unphysical or dangerous modes are removed.

Sensitivity to initial conditions:

A fundamental and far-reaching property of the equations governing atmospheric motion is the sensitivity of their solutions to small perturbations in the initial state. Solutions initially very close to each other evolve so that the difference between them is as large as the difference between randomly chosen states of the system.

There is motion in the atmosphere on scales ranging from planetary waves of thousands of kilometers to millimeter-scale turbulent eddies. The initial state for the numerical weather prediction models, however, is obtained from observations of only those scales of motion large enough to be resolved by the observing network. Smaller scales of motion are completely ignored and indeed, through alias error, cause uncertainty in the determination of large scales . Therefore, no matter how accurately a numerical model computes the evolution of the atmospheric motion there remains a fundamental uncertainty in the forecast due to the error in the initial state.

Predictability of the atmosphere:

It has long been realised that the equations of the atmosphere are highly sensitive to perturbations. Small differences in the initial state tend to magnify and finally lead to very dissimilar final states after a period of a few days or at most a couple of weeks. This has lead researchers to speculate about and seek the limits of predictability of the atmosphere. This research is aimed, in part, at finding a time-scale over which even the smallest errors in the initial state would lead to significantly different final states.

Thompson [1] pioneered the study of predictability by examining the behavior of an idealized two dimensional barotropic atmosphere for an initial error that is isotropic and homogeneous. *Lorenz* [2], using a turbulence closure scheme for two-dimensional flow, showed that error initially confined to smallest scales of motion (order of a few meters) 'cascaded' to higher and higher scales, inducing significant errors in the so called "cumulus scales" (2-10 km) within half an hour, in the "synoptic scales" in two days, and in the planetary scales after two weeks.

Kraichnan [3], *Leith* [4] and *Leith* and *Kraichnan* [5] did similar calculations using sophisticated closure schemes. These studies concluded that, in three dimensions, whatever the scale of initial error, the error will grow and finally dominate the large scales of the flow. Thus a three dimensional flow field is not "predictable" for *all* time even if the initial field is known to an arbitrary degree of accuracy.

Studies which use models closer to the real atmosphere have also been done to discern the effect of chosen atmospheric factors on predictability. The effect of Rossby waves, and the Coriolis parameter ('beta'), on error growth in barotropic models was studied by *Basdevant et al.* [6] and by *Holloway* [7]. Both studies agreed that Rossby wave propagation enhances predictability (i.e. slows error growth). *Vallis* [8] found that such increased predictability due to Rossby waves is not found in baroclinic models.

Roads [9] used a two-level quasi-geostrophic model to study predictability in the extended range. He found that it took about 30 days before the forecast skill of the model was about the same as a persistence forecast. *Strauss* [10] also used a two-level quasi-geostropic model to study the effect of baroclinic instability and wave-wave interactions on the predictability.

Similar predictability studies have also been attempted using more complex General Circulation Models(GCM). *Charney et al.* [11], *Smagorinsky* [12] and *Williamson* and *Kasahara* [13], attempted GCM runs with initial conditions that were in some sense close to each other. The doubling time for small errors was found to be quite model dependent. The role of moisture was included in the later GCM studies of *Baede et al.* [14].

Errors in the initial condition :

The studies mentioned above concentrate on one cause of the errors in forecasting i.e. the tendency of the atmosphere to magnify small differences in the initial state. However, even in a

perfect model, the accuracy of a numerical forecast will depend on at least two factors, namely, (a) the growth rate of error as determined by the equations of motion, and (b) the magnitude and scale of the initial error as determined by the accuracy and resolution of the observing network. The first of these sources of error have been studied by those interested in the 'predictability' of the atmosphere. We shall now consider the second.

The process of converting observed data to the initial conditions for a NWP code is essentially one of finding a suitable analytic representation for point-wise data. It is a process of curve-fitting subject to dynamical and statistical constraints. Often, a least-squares type approach is used to achieve this end. However, there are many sources of error on the path from the 'real' initial fields to the initial conditions finally used in the numerical model.

To get a good interpolation function for point-wise data, it is usually necessary to have a systematic distribution of the data-points. However meteorological observation stations have a very uneven distribution over the earth, with large land masses in the world, and the oceans which cover three-fourths of the globe, scarcely represented. Interpolation using unevenly scattered data-points leads to errors in scale, by which energy at a certain length scale is mistakenly attributed to another scale.

Because the weather stations are at least of the order of hundreds of kilometers apart, only the large scale structure of the atmosphere may even be attempted to be captured by observations. However, large-scale motions may only be detected accurately by observations over correspondingly large time-scales. This however

is not generally feasible, especially in the upper-air observations. Therefore, small time-scale behavior may be mistaken for large time-scale behavior, thereby compounding aliasing error problems. The small-scale, high-wave-number, structure of the atmosphere cannot be obtained due to the poor resolution of the observation net-work; and hence a not insignificant portion of the kinetic energy may be ignored even in the best case.

Observation data undergo a detailed processing, which involves checking the location of observations, for gross errors, for hydrostatic consistency, etc. After preliminary error checks, the fields are subjected to *'Objective Analysis'*. The aim of objective analysis is to extract the maximum information from the observations, consistent with climatological records, space correlations between the meteorological variables, etc. This requires a knowledge of the statistical structure of the fields of the variables, which may be analyzed separately as in *univariate* analysis, or together as in *multivariate* objective analysis.

However, objective analysis procedures are generally not enough to provide the initial conditions for an NWP code. In the atmosphere, the wind and pressure fields are in a quasi-geostrophic, quasi-nondivergent state and little energy is associated with the ageostrophic motion. However, the objective analysis schemes generally do not yield mass and motion fields that are in the delicate state of balance that exists in the atmosphere. Consequently, the use of only objectively analyzed data to initialize an NWP model may generate large, spurious inertial-gravity modes, if the model permits such modes. Furthermore, because of numerical errors, computational instabilities , etc , there may be spurious growth of short waves. which if left unchecked could 'blow up'. Even otherwise. it is

usually desirable to eliminate very high wave number components. Therefore, the fields have to undergo a further process of 'initialization' which will eliminate these unphysical and troublesome aspects of the objectively analyzed data.

It may be remarked that the above procedure for generating initial conditions does not actually correct errors in the raw data (other than in locating gross errors). What it actually does is generate fields which are *similar* to the observed ones but which have dynamic and statistical consistency and which will not cause numerical difficulties. Therefore it may be argued that the initialized fields are far from being error-free.

Initial conditions errors versus numerical integration errors:

Since the 1970's there has been a shift in the numerical method used for global atmospheric models from the finite-difference to the spectral method. The spectral method has a number of advantages, primary amongst which is accuracy. This method has the so-called 'exponential' or 'spectral' accuracy which ensures that, for smooth solutions, the error in the spectral representation decreases faster than any finite power of the grid-interval. Thus, as the number of grid-points are increased in the numerical scheme, the accuracy of the representation rises dramatically. Furthermore, in global spectral models, generally a Spherical Harmonics representation is used which ensures that there are no problems of the discontinuity of the dependent variables and their derivatives at the poles.

The principal disadvantage of the spectral representation is that a large amount of arithmetic is necessary to calculate

spectral equations with even a moderate number of retained modes. The transform method described by *Orszag*[15] reduces the number of arithmetic operations (per level, per time-step) from $O(N^4)$ to $O(N^3)$ where N is the spectral truncation number. However, as these many operations have to be done every time-step, increasing N, which undoubtedly increases accuracy rapidly, also extracts a progressively heavy price in the number of computations.

With the developement of these highly accurate numerical methods, a certain imbalance has crept into the use of numerical weather prediction codes. It is much easier, given the rapid rate of increase of the speed and power of the computers, to increase the *formal* accuracy of the numerical integrations performed by the codes, by increasing the number of grid-points, than to increase the accuracy of the initial conditions being fed into them. This increase in the formal accuracy, of course, increases the computational burden. The result is that the computational requirements of NWP codes grow to fill the capacity of the latest and most powerful computers. We may ask : to what purpose? Does improved accuracy of the numerical integration necessarily increase the accuracy of the forecast, given the uncertainty in the initial conditions ? This study seeks a partial answer to this question.

The error in a forecast may be divided into four categories which are mutually independent, i.e, (a) *modelling errors* due to faults in the model, say, by incorrect representation of the physics, (b) *time stepping errors* due to inaccuracies in the temporal integration of the model equations, (c) *resolution errors* caused by inaccurate representation of the spatial fields, and finally (d) *initial condition dependent* (ICD) *errors* caused by incorrect specification of the initial conditions to the problem. We are primarily concerned with the last two types of error in this

study. The aim of this work is to investigate the degree of spectral accuracy that would be sufficient to resolve a numerical simulation of the atmosphere with a specified amount of error in the initial conditions.

We are primarily concerned with a comparison of the resolution errors with the initial condition dependent errors. Say, with a given number of spectral coefficients (N^2, say) we obtain resolution errors which are approximately the same as the expected ICD errors then, because of the exponential accuracy of the spectral method, we can decrease the resolution errors substantially by a moderate increase in N. But as this will only increase resolution accuracy, while leaving the initial condition dependent(and other) error essentially unaffected, it would be pointless to increase N too much; this will only increase the computations for the illusion of greater accuracy. Therefore the optimum value of N, which we will call N_{opt}, will be slightly larger than that value of N at which resolution and ICD errors will be comparable.

As this is a numerical study, we need a numerical model that suits our needs. We have chosen to study simulations of the one-level barotropic vorticity equation. There are two reasons for this choice:

Firstly, the model is a very simple one and requires the least amount of computation for a given number of spectral coefficients. The second reason, which is more compelling, involves the intimate relationship between the predictability of the atmosphere and initial condition dependent (ICD) error. It is clear that for a less predictable model atmosphere there will be a greater rate of divergence of two states starting from almost identical initial

conditions. This means that the same error in the initial conditions will cause greater ICD error in a less predictable model atmosphere than in a more predicable one and *vice-versa*.

Now, the studies of predictability quoted above have established that (a) three dimensional atmospheres are less predictable than two-dimensional ones, and (b) introduction of baroclinicity makes the model atmosphere less predictable. We may conclude that the one-level barotropic model is *more* predictable than the real atmosphere (and more realistic models), and will, therefore, have a less rapid growth of ICD errors. However, the resolution errors in this model will be about the same (for the same number of spectral coefficients per level) as in any other model. In comparing the resolution and ICD errors in a barotropic model we will, therefore, be *underestimating* the relative magnitude of the latter (with reference to a more realistic model of the atmosphere). Therefore the optimum resolution N_{opt}, which is chosen such that the resolution errors are dominated by the ICD, will be an ***overestimate***. Therefore, in using the barotropic model we are finding the *upper limit* of the spectral resolution required in NWP codes.

The approach that is followed in this study is similar to the 'identical twin' numerical experiments that are so common in predictability studies. First, certain 'standard' initial conditions are selected. The highest resolution calculations of the evolution of the model atmosphere, using these standard initial conditions, are treated as the 'exact solution'. Other simulations, done using either (a) coarser grids (poorer resolution) or (b) erroneous initial conditions, are compared with the exact solution to determine resolution errors and ICD errors, respectively. Error

in the initial conditions is introduced by randomly perturbing the initial spectral coefficients from the 'standard' values. Uniformly distributed random numbers are used to generate errors of any chosen standard deviation. In other simulations, the error is introduced in low, and high, wavenumber initial spectral coefficients, respectively, to assess the wavenumber dependence of the rate of growth of the initial error.

The barotropic model is one of the oldest numerical models of the atmosphere and has been studied extensively. Detailed explanation of the spectral form of this equation and the numerical technique used in solving it are given, for example, in *Haltiner* and *Williams* [16], *Holton* [17], and in *Washington* and *Parkinson*[18].

The thesis contains a detailed discussion of the derivation of the nondivergent barotropic vorticity equation, an introduction to the spectral method, spherical harmonics, and the energy spectra of scalar fields in chapter 2. Chapter 3 contains a description of the non-dimensionalization of the barotropic vorticity equation, its spectral formulation , and the algorithm used in the present work. Finally, chapter 4 lists out the results and related discussions.

CHAPTER TWO

THE METHOD

This chapter contains the details of the methods implemented in the present work. The topics covered include the derivation of the synoptic scale momentum equation in spherical coordinates, the Barotropic vorticity equation, the discrete Fourier transform. Associated Legendre polynomials, Gaussian-quadrature, Aliasing, and Spherical Harmonics.

(2.1) Primitive Equations

Atmospheric motions are governed by the principles of conservation of mass, momentum, and energy. The momentum equation relates the rate of change of momentum (i.e. the *total* time derivative of momentum) in an inertial reference frame to the sum of the forces acting on the fluid. By the total time derivative of a quantity (also called the Lagrangian derivative) is meant the rate of change of that quantity as *seen by a particle of the moving fluid*. This is related to the time and space derivatives as seen by a stationary observer in the following manner:

$$\frac{d}{dt} = \frac{\partial}{\partial t} + u \frac{\partial}{\partial x} + v \frac{\partial}{\partial y} + w \frac{\partial}{\partial z}$$

where u, v, and w are the component velocities in x, y, and z directions respectively. The quantity on the left side of the equation is the total derivative; the first quantity on the right is called the *local* derivative and the last three terms are

is called the *local* derivative and the last three terms are called the *convection* or *advection* terms (which are often denoted by the notation $\hat{V}\cdot\nabla$).

In meteorology it is desirable to describe the motion in a reference frame rotating with the earth. The transformation of the total time derivative of a vector $\hat{A}$ in an inertial frame and the corresponding total derivative in a rotating system with constant angular velocity Ω is

$$\left.\frac{d\hat{A}}{dt}\right)_{inertial} = \left.\frac{d\hat{A}}{dt}\right)_{rotating} + \hat{\Omega}\times\hat{A} \qquad (2.1.1)$$

In an inertial frame Newtons second law of motion may be written symbolically as

$$\left.\frac{d\hat{U}}{dt}\right)_{inertial} = \Sigma\,\hat{F} \qquad (2.1.2)$$

The left hand side represents the rate of change of the absolute velocity $\hat{U}$ following the motion as viewed in an inertial system. The right-hand side represents the sum of the real forces acting per unit mass. By applying (2.1.1) to the position vector $\hat{r}$ for an air parcel on the rotating earth we get :

$$\left.\frac{d\hat{r}}{dt}\right)_{inertial} = \left.\frac{d\hat{r}}{dt}\right)_{rotating} + \hat{\Omega}\times\hat{r} \qquad (2.1.3)$$

The first term on the RHS of (2.1.3) is the velocity of the particle with respect to the rotating system which will be denoted by $\hat{U}_a$. We can then rewrite (2.1.3) as

$$\hat{U}_a = \hat{U} + \hat{\Omega}\times\hat{r} \qquad (2.1.4)$$

which states simply that the absolute velocity of an object on the rotating earth is equal to its velocity relative to the earth plus the velocity due to rotation of the earth.

Next we apply (2.1.1) to the velocity vector $\hat{U}_a$ and obtain

$$\left.\frac{d\hat{U}_a}{dt}\right]_{inertial} = \left.\frac{d\hat{U}}{dt}\right]_{rotating} + \hat{\Omega} \times \hat{U}_a \qquad (2.1.5)$$

Substituting from (2.1.4) into the right-hand side of (2.1.5) we get

$$\left.\frac{d\hat{U}_a}{dt}\right]_{inertial} = \frac{d(\hat{U} + \hat{\Omega} \times \hat{r})}{dt} + \hat{\Omega} \times (\hat{U}_a \times \hat{r})$$

$$= \frac{d\hat{U}}{dt} + 2\,\hat{\Omega} \times \hat{U} - \Omega^2 R \qquad (2.1.6)$$

where the last expression on the R.H.S. is in the rotating system. Here R is the projection of $\hat{r}$ on a plane perpendicular to the axis of rotation, Therefore the acceleration of a body with respect to an inertial system equals its acceleration in a rotating system plus the coriolis and centripetal acceleration terms. The second and third term on the RHS of (2.1.6) are called coriolis and centripetal acceleration respectively. These are called 'fictitious' acceleration terms because their existence is solely due to the fact that motion is being observed from a non-inertial frame.

If we assume that the only 'real' forces acting on the atmosphere are the pressure gradient force, gravitation, and friction, we can rewrite Newtons second law (2.1.2) as

$$\frac{d\hat{U}}{dt} = - 2\,\hat{\Omega} \times \hat{U} - (1 / \rho)\,\nabla P + \hat{g} + \hat{F}r \qquad (2.1.7)$$

where $\hat{F}r$ designates the friction force, P is the pressure and the centripetal force has been combined with gravitation in the gravity term $\hat{g}$. Equation (2.1.7) is the fundamental form of momentum equation dynamic meteorology.

(2.2) The Component equations in Spherical coordinates

The shape of the earth is nearly spherical, therefore it is convenient to expand (2.1.7) in spherical coordinates. The coordinates are then (λ,ϕ,Z), where λ is the longitude, ϕ is the latitude and Z is the vertical distance above the surface of the earth. If the position of an object is denoted by (λ,ϕ,Z) and if the unit vectors $\hat{i}$, $\hat{j}$, $\hat{k}$ are now taken to be directed eastward (increasing λ), northward (increasing ϕ), and upward (increasing Z), respectively, the relative velocity of the object with respect to the earth is

$$\hat{U} \equiv \hat{i}\,u + \hat{j}\,v + \hat{k}\,w$$

where the components u, v, and w are defined as

$$u \equiv r\cos\phi\,\frac{d\lambda}{dt}\,, \quad v \equiv r\,\frac{d\phi}{dt}\,, \quad w \equiv \frac{dz}{dt} \qquad (2.2.1)$$

Here , r is the distance to the center of the earth which is related to z by r = a+ z, where a is radius of the earth. Generally, the variable r in (2.2.1) is replaced by the constant a. This is a very good approximation since $z \ll a$ for the regions of the atmosphere with which meteorologis t is concerned . For

convenience, meteorologists have traditionally used a coordinate system which is spherical in nature but which is cartesian-like over small distances. This is done by defining a coordinate x as the eastward distance and y as the northward distance from a given point ($dx = a \cos\phi \, d\lambda$, $dy = a \, d\phi$). For small areas, as the curvature of the earth has negligible effect, the coordinates x and y essentially define a locally cartesian system. The velocity components can be expressed as $u \equiv (dx/dt)$, $v \equiv (dy/dt)$, and $w \equiv (dz/dt)$ and the unit vectors $\hat{i}$, $\hat{j}$, $\hat{k}$ are in the x, y, and z directions, respectively. However the system is not cartesian as $\hat{i}$, $\hat{j}$, and $\hat{k}$ depend on the location of the point (x, y, z). This position dependence of the unit vectors must be taken into account when the acceleration vector is expanded into its components on the sphere. Thus we write

$$\frac{d\hat{U}}{dt} = \hat{i}\frac{du}{dt} + \hat{j}\frac{dv}{dt} + \hat{k}\frac{dw}{dt} + u\frac{d\hat{i}}{dt} + v\frac{d\hat{j}}{dt} + w\frac{d\hat{k}}{dt} \qquad (2.2.2)$$

where $$\frac{d\hat{i}}{dt} = u\frac{\partial \hat{i}}{\partial x} = u\frac{1}{a\cos\phi}(\hat{j}\sin\phi - \hat{k}\cos\phi) \qquad (2.2.2a)$$

$$\frac{d\hat{j}}{dt} = u\frac{\partial \hat{j}}{\partial x} + v\frac{\partial \hat{j}}{\partial y} = -u\frac{\tan\phi}{a}\hat{i} - \frac{v}{a}\hat{j} \qquad (2.2.2b)$$

$$\frac{d\hat{k}}{dt} = \frac{u}{a}\hat{i} + \frac{v}{a}\hat{j} \qquad (2.2.2c)$$

Substituting equation (2.2.2) into (2.1.7) and equating components on the left and right hand side of the resulting equation we get

$$\frac{du}{dt} - \frac{u\,v\tan\phi}{a} + \frac{u\,w}{a} = -\frac{1}{\rho}\frac{\partial p}{\partial x} - 2\Omega\, w\cos\phi + 2\Omega\, v\sin\phi + F_x \qquad (2.2.3)$$

$$\frac{dv}{dt} + \frac{u^2 \tan\phi}{a} + \frac{vw}{a} = -\frac{1}{\rho}\frac{\partial p}{\partial y} - 2\,\Omega\,u\sin\phi + Fy \qquad (2.2.4)$$

$$\frac{dw}{dt} - \frac{u^2 + v^2}{a} = -\frac{1}{\rho}\frac{\partial p}{\partial z} - g + 2\,\Omega\,u\cos\phi + Fz \qquad (2.2.5)$$

where Fx, Fy, and Fz are the three components of the frictional force. The terms proportional to 1/a on the LHS in (2.2.3)-(2.2.5) (which are called the curvature terms because they arise due to curvature of the earth) are non-linear. Although, as will be shown in the next section, the curvature terms are unimportant for mid latitude synoptic scale motions and may be neglected, (2.2.3)-(2.2.5) are still non-linear PDEs as can be seen by expanding the total derivatives into their local and advective parts. In general the non-linear advective acceleration terms are comparable in magnitude to the linear local acceleration terms. It is primarily the presence of non-linear advection processes that causes the rich and complex behavior of the atmosphere.

(2.3) Scale analysis of Equation of Motion

The equations of motion derived in the last section are complicated coupled non-linear PDE's. A natural hope that arises is that a way may be found to simplify them. This may be done by evaluating the order of magnitude of the various terms in the equations and neglecting those that are small in comparison to others. This approach has been found to be very fruitful in meteorology and often leads to a substantial reduction in the number of terms in the equations. This kind of order of magnitude analysis is called *scale analysis* or *scaling*.

In scaling, typical values of the magnitude of the field variables, and the amplitude of their fluctuations, and the characteristic length, depth and time-scales are estimated. These typical values are then used to determine the magnitude of various terms in the governing equations.

The character of the atmospheric motions depends very strongly on the horizontal scale. Table (2.1) presents various types of motions classified by horizontal scale for the spectral region from 10^{-7} to 10^{7}m.

TABLE- 2.1

Types of motion	Horizontal scale(m)
Molecular mean free path	10^{-7}
Minute turbulent eddies	10^{-2}-10^{-1}
Small eddies	10^{-1}-1
Dust devils	1-10
Gusts	10-10^{2}
Tornadoes	10^{2}
Cumulonimbus	10^{3}
Fronts	10^{4}-10^{5}
Hurricanes	10^{5}
Synoptic cyclones	10^{6}
Planetary waves	10^{7}

Elimination of terms by scaling not only simplify the athematics, but in some cases it completely eliminates, or ilters, unwanted type of motions. For example, in an analysis of urricanes (~10^{5} m) we are usually not interested in motion of the

›rder of 10^2m (gusts) and these may be filtered out of the ›quatıons by scaling.

The term *synoptic* is associated with the analysis of ›bservations taken over a wide area at or near the same time. The ynoptic scale ıs the characteristic scale of dısturbances which re depicted on weather maps(10^6m). In order to simplify 2.2.3)-(2.2.5) for synoptıc scale motions we define the followıng ypical values of variables based on observed values for id latitude synoptic systems.

$U \sim 10$ m s^{-1} horizontal velocity scale
$W \sim 1$ cm s^{-1} vertical velocity scale
$L \sim 10^6$ m length scale [$\sim 1/(2\pi)$ wavelength]
$D \sim 10^4$ m depth scale
$\Delta p/\rho \sim 10^8$ m^2 s^{-2} horizontal pressure fluctuation scale
$L/U \sim 10^5$ s time scale

› take a typical value of the latitude as $\phi_o = 45^o$ and estimate ıe coriolis parameter $f \equiv 2\Omega \sin\phi \simeq 10^{-4}$ s^{-1}. Now we can estimate ıe magnitude of each term in the equation (2.2.3)-(2.2.5) by ›placing each variable by its typical value and replacıng ›rivatives by the ratio of the typical values of the fferentiated variable and the differentiating variable. Table :.2) shows the typical magnitude of each term in (2.2.3) and :.2.5) obtained by this procedure.

Frictional terms are neglected because, for synoptic time ales, frictional dissipatıon is significant only ın the regıon ry near the surface of the earth. From table(2.2) ıt is clear at the coriolis force and the pressure gradıent force are of the eatest magnitude while the other terms are ınsignıficant ın

comparison. Therefore, retaining only these two terms in (2.2.3) and (2.2.4), we obtain as a first approximation the *geostrophic* relationship

$$f\,v \simeq \frac{1}{\rho}\frac{\partial p}{\partial x}\,, \qquad f\,u \simeq -\frac{1}{\rho}\frac{\partial p}{\partial y} \tag{2.3.1}$$

where $f \equiv 2\Omega_e \sin\phi$ is called Coriolis parameter. The geostrophic expression gives the approximate relationship between the pressure field and horizontal velocity in synoptic scale systems. However it contains no reference to time, and therefore cannot be used to predict the evolution of the velocity field. It for this reason that geostrophic relationship is called a *diagnostic* relationship.

To obtain a prediction equation it is necessary to retain the acceleration term in (2.2.8) and (2.2.9) .The resulting approximate horizontal momentum equations are

TABLE- 2.2 Scale-analysis of Horizontal Momentum Equations

x and y momentum equations are :

$$\frac{du}{dt} - \frac{u\,v\,\tan\phi}{a} + \frac{u\,w}{a} = -\frac{1}{\rho}\frac{\partial p}{\partial x} - 2\,\Omega_e\,w\cos\phi + 2\,\Omega_e\,v\sin\phi$$

$$\frac{dv}{dt} + \frac{u^2\tan\phi}{a} + \frac{vw}{a} = -\frac{1}{\rho}\frac{\partial p}{\partial y} - 2\,\Omega_e\,u\sin\phi$$

Scale of individual terms :

U^2/L	U^2/a	UW/a	$\Delta P/(\rho L)$	$f_o W$	$f_o U$
Magnitude of terms($m\,s^{-2}$):					
10^{-4}	10^{-5}	10^{-8}	10^{-3}	10^{-6}	10^{-3}

$$\frac{du}{dt} - f\,v = -\frac{1}{\rho}\frac{\partial p}{\partial x} \qquad (2.3.2)$$

$$\frac{dv}{dt} + f\,u = -\frac{1}{\rho}\frac{\partial p}{\partial y} \qquad (2.3.3)$$

As table (2.2) shows, the acceleration terms are about an order of magnitude smaller than the coriolis force and pressure gradient force. Thus,a small error in measurement of either velocity or pressure gradient will lead to very large error in estimating the acceleration by using the above equations.

(2.4) Barotropic Vorticity Equation

The equations (2.3.2) and (2.3.3) may be used to develop a very simple model of the atmosphere called the *Barotropic* model. This model assumes that the velocity field above a point (x,y) can be represented by a single value, i.e. it ignores the vertical variation of the vertical variation of the velocity field and approximates a 3-D field by a 2-D one. A further assumption in the model is that the 2-D velocity field is incompressible and frictionless. Physically, these assumptions equate the atmosphere to an inviscid barotropic fluid i.e. one in which density is a function of pressure alone (and independent of say, temperature). It has been found that at any given time, significant portions of the atmosphere indeed exhibit nearly barotropic behavior. The model is, therefore, not as unphysical as it may at first appear.

Flow fields can be decomposed into the sum of two vectors: one nondivergent(incompressible) but with vorticity, the other divergent(compressible) but irrotational. For large-scale weather patterns in mid-latitudes, the nondivergent, rotational vector is

usually by far the larger of the two, so that by studying vorticity we are studying a representation of most of the flow. It is well known that the motion of a 2-D incompressible fluid can be represented by a single scalar function called the stream function. The stream function, by its very existence, ensures that the velocity field described, complies with the incompressibility condition. Therefore, there is no need to solve the continuity equation if a stream function formulation is used. The two momentum equations for u and v velocity are replaced by two scalar equations relating stream function and vorticity which will provide an equivalent description of the motion. (Vorticity is a vector for a 3-D field but in 2-D it has only one non-zero component and can hence be regarded as a scalar). The velocity u and v can be easily obtained from the stream function if needed.

The vorticity equation can be derived using the momentum equations (2.3.2) and (2.3.3) . We differentiate the x component equation with respect to y and y component equation with respect to x :

$$\frac{\partial}{\partial y}\left\{\frac{\partial u}{\partial t} + u\frac{\partial u}{\partial x} + v\frac{\partial u}{\partial y} + w\frac{\partial u}{\partial z} - f v = -\frac{1}{\rho}\frac{\partial p}{\partial x}\right\} \qquad (2.4.1)$$

$$\frac{\partial}{\partial x}\left\{\frac{\partial v}{\partial t} + u\frac{\partial v}{\partial x} + v\frac{\partial v}{\partial y} + w\frac{\partial v}{\partial z} - f v = -\frac{1}{\rho}\frac{\partial p}{\partial y}\right\} \qquad (2.4.2)$$

Subtracting (2.4.1) from (2.4.2) and defining the (vertical component of) vorticity $\zeta = (\partial v/\partial x) - (\partial u/\partial y)$ we obtain the vorticity equation [using the fact that the Coriolis parameter depends only on y so that $df/dt = v\,(df/dy)$]

$$\frac{d(\zeta + f)}{d t} = - (\zeta + f) \left(\frac{\partial u}{\partial x} + \frac{\partial v}{\partial y} \right) - \left(\frac{\partial w}{\partial x} \frac{\partial v}{\partial z} - \frac{\partial w}{\partial y} \frac{\partial u}{\partial z} \right)$$

$$+ (1/\rho^2) \left(\frac{\partial \rho}{\partial x} \frac{\partial p}{\partial y} - \frac{\partial \rho}{\partial y} \frac{\partial p}{\partial x} \right) \qquad (2.4.3)$$

The three terms on the right of (2.4.3) are called the divergence term, the tilting term or the twisting term , and the solenoidal term, respectively.

Equation (2.4.3) can also be simplified using scale analysis. For synoptic scale motions we can choose the same characteristic scales as given in section (2.3).

$U \sim 10$ ms^{-1} horizontal velocity scale
$W \sim 1$ $cm\ s^{-1}$ vertical velocity scale
$L \sim 10^6$ m length scale [$\sim 1/(2\pi)$ wavelength]
$D \sim 10^4$ m depth scale
$\delta p \sim 1$ kPa horizontal pressure fluctuations
$\rho \sim 1$ kg m^{-3} mean density
$\delta\rho/\rho \sim 10^{-2}$ fractional density fluctuation
$\Delta p/\rho \sim 10^3\ m^2 s^{-2}$ horizontal pressure fluctuation scale
$L/U \sim 10^5$ s time scale
$f_o \sim 10^{-4}$ coriolis parameter
$df/dy \equiv \beta \sim 10^{-11}$ "beta" parameter

Using these scales to evaluate the magnitude of the terms in (2.4.3) we note that

$$\zeta \sim 10^{-5} \quad s^{-1}$$

$$f \left(\frac{\partial u}{\partial x} + \frac{\partial v}{\partial y} \right) \sim 10^{-6}$$

$$\zeta \left(\frac{\partial u}{\partial x} + \frac{\partial v}{\partial y} \right) \sim 10^{-10}$$

$$\left(\frac{\partial w}{\partial x} \frac{\partial v}{\partial z} - \frac{\partial w}{\partial y} \frac{\partial u}{\partial z} \right) \sim 10^{-11}$$

$$(1/\rho^2) \left(\frac{\partial \rho}{\partial x} \frac{\partial p}{\partial y} - \frac{\partial \rho}{\partial y} \frac{\partial p}{\partial x} \right) \sim 10^{-11}$$

Retaining now only the term of order 10^{-10} s^{-2} in the vorticity equation, we obtain as the first approximation for synoptic scale motions

$$\frac{d(\zeta + f)}{d t} = - (\zeta + f) \left(\frac{\partial u}{\partial x} + \frac{\partial v}{\partial y} \right) \qquad (2.4.4)$$

As a first approximation the change of absolute vorticity following the horizontal motion on the synoptic scale is entirely due to divergence effect .

BAROTROPIC MODEL :

We use the one parameter Barotropic model for our study. By one parameter model is meant that the model uses only one data point in the vertical direction. The assumptions in the *Barotropic model* are

(1) Inviscid and incompressible flow.

(2) Motion is two-dimensional (vertical motion is altogether neglected).

(3) Effect of frictional forces is neglected.

Then vorticity equation becomes

$$\frac{d(\zeta + f)}{d t} = 0$$

or $$\frac{\partial \zeta}{\partial t} = - \hat{U} \cdot \nabla (\zeta + f) \qquad (2.4.5)$$

Note $\hat{U}$ in the case of barotropic flow will consists of only nondivergent part of the velocity field. Furthermore, as only one level is allowed , we may represent the velocity field at some chosen isobar(say 300 or 500 mb) where the field is nearly divergenceless.

The barotropic model is a useful approximate forecast equation for short range weather predictions. To a limited extent model is used to understand the basic idealized properties of large scale dynamical motions.

(2.5) Spectral Method

Spectral method are global approximations unlike, finite difference methods which make approximations of, say,the derivative of a function by using the nearest neighbors. The spectral approach is to fit a function through all the grid points and use this to find the derivative at any point.

The essence of the spectral method lies in the approximation of functions by a truncated series of standard known functions called trial functions. The expansion of a function A(x) would be of the form

$$A_{app}(x) = \sum_{N} A_n Z_n(x) \qquad , a \leq x \leq b \qquad (2.5.1)$$

where $A_{app}(x)$ is the spectral approximation to A(x) and A_n's are (complex) constants called spectral coefficients. $Z_n(x)$ is a trial function. The wave number n varies from 0 to N-1 [or from (N/2)-1 to N/2 depending on the type of trial function] where N is the total number of terms in the series.

The commonly used trial functions are

(a) Fourier
(b) Chebyshev
(c) Legendre
(d) Spherical harmonics
(e) Hermite
(f) Laguerre .

The trial functions are orthogonal functions. Not all the trial function sets will give infinite order accuracy but the ones named above will do so. By "Infinite order accuracy" is meant that the error in the expansion will fall faster than any any polynomial of (1/N) as N-->∞. It is also called "exponential" and "Spectral" accuracy. The choice of the sets of trial functions depends on the problem. Fourier functions can only be used for expansion of periodic functions, while spherical harmonics can only be used for the expansions in a spherical coordinate system. Chebyshev functions are suitable for finite domain (rectangular) problems. The choice of function set is also dependent on the availability of efficient algorithm to evaluate spectral coefficients A_n for any given function A(x).

(2.5.a) Evaluation of coefficients

Obviously, the crux of finding good approximations for A(x) in equation (2.5.1) lies in finding the the best values of (the as-yet-unknown) spectral coefficients. This is where the orthogonal property of the trial functions are useful. We can utilize the orthogonal property of the trial function to find spectral coefficients A_n.

If the trial function Z_n's satisfy the following orthogonality relations

$$\int_a^b \omega(x)\, Z_n(x)\, Z_m(x)\, dx = \delta_{mn} \qquad (2.5.2)$$

where $\omega(x)$ is a weight function and δ_{mn} is the Dirac-Delta function. Then by multiplying (2.5.1) by $w(x)Z_m(x)$ (where $0 \le m \le N-1$) and integrating between the limits a to b we get

$$\int_a^b w(x)\, A(x)\, Z_m(x)\, dx = \sum_{n=0}^{N-1} \int_a^b \omega(x)\, A_n\, Z_n(x)\, Z_m(x)\, dx$$

$$= \sum_{n=0}^{N-1} A_n\, (C_n\, \delta_{nm})$$

As m is between 0 to N-1 this sum will have only one non-zero term when n=m. Therefore the sum will be equal to $A_n C_n$ and

$$A_n = \frac{1}{C_n} \int_a^b w(x)\, A(x)\, Z_n(x)\, dx \qquad (2.5.3)$$

From equation (2.5.3) it can be seen that given a function A(x) and a set of orthogonal trial function Z_n's. We can find the coefficients A_n for the approximate spectral expansion of A(x) by integration. However, in the usual applications of spectral methods these integration will have to be done a very large number of times; hence to do them analytically is out of the question. Generally, therefore, a numerical quadrature rule is used for the integration in equation (2.5.3).

(2.5.b) Gaussian Quadrature

The gaussian quadrature rules are the most accurate in evaluating integrals by numerical integration .The accuracy of these method is a great jump over that of the regular interval quadratures because with N points we get 2N-1 polynomial accuracy. The idea of the gaussian quadrature is to get a good approximation of an integral by weighted sum of the function values at certain specially chosen points i.e.

$$\int_a^b \omega(x)\, A(x)\, dx \simeq \sum_{i=0}^{N-1} w_i\, A(x_i) \qquad (2.5.4)$$

where $\omega(x)$ is a weight function of the orthogonal set $Z_n(x)$, the $A(x_i)$ the function values at grid points x_i's and w_i's are the weights assigned to those function values.

The collocation points (also called the grid points) x_i's and weights w_i that give the most accurate evaluation of the integrals depend on the weight function $\omega(x)$ and the limits a , b of the integral. Depending on the weight function $\omega(x)$ used in the integral, we get various different quadratures like Gauss-Legendre, gauss- Chebyshev etc. and different corresponding collocation points.

For an N point Gaussian quadrature the collocation points are chosen as the zeros of the N^{th} order trial function $Z_N(x)$. It can be proved that these points get the highest order accuracy for a general integrand. In case of spherical harmonics(a trial function consisting of product of Legendre and Fourier terms), we have evenly spaced grids in the longitudinal direction(zeros of Fourier component) and unevenly spaced in meridional direction (zeros of

associated Legendre polynomial).

The weight functions of the quadrature can be obtained by demanding that (2.5.4) be exact if A(x) is any of the orthogonal set $Z_0(x), Z_1(x), \ldots\ldots\ldots\ldots, Z_{N-1}(x)$. This means

$$w_0 Z_0(x_0) + w_1 Z_0(x_1) + \quad + w_{N-1} Z_0(x_{N-1}) = \int_a^b w(x)\, Z_0\, dx$$
$$w_0 Z_1(x_0) + w_1 Z_1(x_1) + \quad + w_{N-1} Z_1(x_{N-1}) = \int_a^b w(x)\, Z_1\, dx$$
$$\ldots\ldots\ldots\ldots\ldots\ldots\ldots\ldots\ldots\ldots\ldots\ldots\ldots\ldots\ldots\ldots$$
$$w_0 Z_{N-1}(x_0) + w_1 Z_{N-1}(x_1) + \quad + w_{N-1} Z_{N-1}(x_{N-1}) = \int_a^b w(x)\, Z_{N-1}\, dx$$

Writing the above equations in matrix form ,we have

$$\left[Z \right] \left\{ w \right\} = \left\{ C \right\} \qquad (2.5.5)$$

As $x_0, x_1, \ldots\ldots\ldots, x_{N-1}$ are known (i.e. roots of the N^{th} order trial function) the matrix [Z] and column vector {C} are also known. Thus by solving the matrix equation (2.5.5) ,we can easily determine weight functions of the quadrature i.e. {w}.

Once the collocation points and weights are found for the quadrature to evaluate the integral (2.5.3), we can develop a relationship between function values at grid points and the spectral coefficients.

Given that the values at the x_j collocation point is A_j we see that the application of the Gaussian quadrature to (2.5.3) will yield

$$A_n = \frac{1}{Cn} \sum_{j=0}^{N-1} w_j A_j Z_n(x_j) \qquad (2.5.6)$$

which is called a "forward transform". Also given the values of the coefficients A_n we can evaluate the values at the grid points A_j by using (2.5.1) to get

$$A_j = \sum_{n=0}^{N-1} A_n \, Z_n(x_j) \qquad (2.5.7)$$

(2.5.c) Discrete Fourier Transform

For a periodic function A(x) { $0 \leq x \leq L$} there exists a finite transform called the discrete Fourier transform which relate the spectral coefficients A_k of the expansion

$$A_{app}(x) = \sum_{k=0}^{N-1} A_k \; e^{i\left(\frac{2\pi}{L}\right) k x} \qquad (2.5.8)$$

with the values of A(x) at the collocation points x_j. These collocation points are defined as

$$x_j = (j\,L)/\,N \qquad j=0,1,\ldots\ldots,N-1 \qquad (2.5.9)$$

The collocation points x_j are evenly spaced .

If A_j is the set of functions values at the collocation points x_j then

$$A_k = \frac{1}{N} \sum_{j=0}^{N-1} A_j \; e^{-(2\pi i k j/N)} \qquad \text{for } k=0,1,2,\ldots\ldots,N-1 \qquad (2.5.10)$$

and the inverse transform is

$$A_j = \sum A_k \; e^{(2\pi i j k/N)} \qquad j=0,1,\ldots\ldots\ldots,N-1 \qquad (2.5.11)$$

Generally these summations in equations (2.5.10) and (2.5.11) are never done by a straight forward evaluation. The Fast Fourier Transform(an ingenious algorithm) is used for its evaluation. A straight forward evaluation takes $O(N^2)$ operations while a FFT takes only $O[N \ln_2(N)]$ which is much smaller (for larger values of N).

The FFT is a particular way of factorizing and rearranging the terms in the sums of the discrete Fourier transform.

(2.6) .Aliasing

In the spectral approximation generally the lowest-order coefficients are the largest and therefore most important. Therefore the larger the value of k less will be the significance of the corresponding coefficients. Given that two functions $f_N(x)$, $g_N(x)$ are represented by their values at the grid or collocation points, how should their product $h_N(x)=f_N(x)\ g_N(x)$ be evaluated ? The obvious answer is that the value of $h_N(x)$ at the collocation points be obtained by multiplying the corresponding values of $f_N(x)$ and $g_N(x)$ at the same collocation points, i.e.

$$h_j = f_j\ g_j \qquad , \ j= 1,.....,N \qquad (2.6.1)$$

However there is a subtle reason why this approach is not altogether right. The approximate functions $f_N(x)$ and $g_N(x)$ are (N-1)th order polynomials and if their values at N collocation points is known the finite transform will exactly evaluate their corresponding coefficients. However if a polynomial of order greater than N-1 is represented on only N collocation points, the finite transform will no longer be able to evaluate the

coefficients exactly. All the coefficients will be have some error.

If $f_N(x)$ and $g_N(x)$ are $(N-1)^{th}$ order polynomials then obviously their product $h_N(x)$ will be of order 2N-2 . If $h_N(x)$ is represented by only N points there will be some error in the evaluation of the coefficients of $h_N(x)$. This error is called *aliasing* error and effects both the low order important coefficients and the less important higher order coefficients.

However, if $f_N(x)$ and $g_N(x)$ are polynomials of order (N-1)/2 each we can see that $h_N(x)$ will be polynomial of order N-1 and its coefficients can be evaluated exactly. This is done by finding coefficients from the collocation point values (f_j, g_j) and putting the upper half of the coefficients to zero to get the function values (f_j^e, g_j^e) at the collocation points. These function values will not be the original function values but will correspond to a polynomial of one-half the original order (because the upper half coefficients are put to zero). Therefore f_j^e and g_j^e are " smoothened " values of the original values f_j and g_j, and h_j is evaluated by

$$h_j = f_j^e \; g_j^e \qquad , \; j= 1 \; ,2 \; ,.....,N \qquad (2.6.2)$$

As we know that the upper coefficients are the least significant and hence ignoring them will introduce the least error. In the original procedure of equation (2.6.1), the error affected all the coefficients of $h_N(x)$ but in the second procedure (which is called truncation of modes) the lower half of the $h_N(x)$ coefficients are exactly evaluated and the error is confined to the upper (less significant) coefficients.

(2.7) Spherical Harmonics

For our purposes, spherical harmonics may be thought of as generalized Fourier Series applicable to the globe. The spherical harmonics have a number of useful properties that explain its wide spread use in the expansion of functions defined on a sphere. Namely, Spherical Harmonics (and its derivatives) are periodic in the longitudinal direction and are single valued and continuous at the poles. For infinitely smooth functions they also are spectral trial function i.e. the error in an expansion of a Spherical Harmonics drops off exponentially as the number of terms are increased.

The spherical harmonic functions are functions of latitude(ϕ) and longitude(λ). The order of the spherical harmonics is characterized by a pair of integers (n, m). Spherical harmonics are so named because they are defined over the surface of a sphere and because solutions of Laplace's equation were called *harmonic* functions. Each Spherical Harmonic is the solution of the angular part of the Laplace equation.

$$Y_n^m(\lambda,\mu) = P_n^m(\mu)\, e^{i\, m_\alpha\, \lambda} \qquad (2.7.2)$$

where

$$\mu \equiv \sin\phi \qquad (2.7.3)$$

Spherical harmonics are therefore the product of the associated Legendre polynomial $P_n^m(\mu)$ and the complex exponential(Fourier component) $e^{im_\alpha\lambda}$.

(2.7.a) Associated Legendre Polynomials

Because of their convenient properties for treating the latitude variation on a sphere, Associated Legendre Polynomials are often used in global atmospheric models.

The associated legendre polynomials may be represented by

$$P_n^m(\mu)=\left\{\frac{(2n+1)\ (n-m)!}{2\qquad (n+m)!}\right\}^{1/2}\frac{(1-\mu^2)^{m/2}}{2^n(n)!}\frac{d^{m+n}}{d\mu^{m+n}}(\mu^2-1)^n \qquad (2.7.3)$$

In this representation the functions are normalized as well as orthogonal i.e.

$$\int_{-1}^{1} P_n^m\ P_k^m\ d\mu = \delta_n^k \qquad (2.7.4)$$

The function $P_n^m(\mu)$ has the following properties

(1) There are n-m zeros of the function between the poles($\mu=\pm1$).

(2) Only the P_n^0 are non-zero at the poles.

(3) Those functions for which n+m is even are even (i.e. symmetric) and those for which n+m is odd are antisymmetric in μ.

(2.7.b) Recursive relations for Spherical Harmonics

For the the spherical harmonics $Y_n^m = P_n^m\ e^{\iota m\lambda}$ there are number of relations. In particular

$$Y_n^m = 0 \qquad , \quad n < m \tag{2.7.13}$$

$$Y_n^{-m} = (-1)^m \; Y_n^{m\,*} \tag{2.7.14}$$

$$Y_n^m = (-1)^{n+m} \; Y_n^m \tag{2.7.15}$$

$$Y_{n+1}^n = \sqrt{(2n+3)}\;\mu\; Y_n^n \tag{2.7.16}$$

$$Y_{n+1}^m\; \varepsilon_{n+1}^m = \mu\; Y_n^m - Y_{n-1}^m\; \varepsilon_n^m \tag{2.7.17}$$

$$Y_{n+1}^{n+1} = \left[\frac{2n+3}{2n+2}\right]^{1/2} (1-\mu^2)^{1/2}\; e^{i\lambda}\; Y_n^n \tag{2.7.18}$$

The derivative of spherical harmonics along zonal direction is given by the relation

$$\frac{\partial\, Y_n^m}{\partial\, \lambda} = i\, m\, Y_n^m \tag{2.7.19}$$

The derivative of Y_n^m along meridional direction is given by

$$(1-\mu^2)\;\frac{\partial\, Y_n^m}{\partial\, \mu} = -\,n\;\varepsilon_{n+1}^m\; Y_{n+1}^m + (n+1)\;\varepsilon_n^m\; Y_{n-1}^m \tag{2.7.20}$$

The laplacian of Y_n^m is a extremely simple relation

$$\nabla^2 Y_n^m = -\,\frac{n\,(n+1)}{a^2}\,Y_n^m = -\,\frac{C_n}{a^2}\,Y_n^m \tag{2.7.21}$$

where $$\nabla^2 = \frac{1}{a^2\,\cos\phi}\left[\frac{\partial}{\partial\,\phi}\cos\phi\frac{\partial}{\partial\phi} + \frac{1}{\cos\phi}\,\frac{\partial^2}{\partial\,\lambda^2}\right] \tag{2.7.22}$$

It can be seen from (2.7.21) that Spherical Harmonics are eigen functions of the laplacian operator defined on a sphere.

The orthogonality relationship for the spherical harmonics is given by

$$\frac{1}{2\pi}\int_{0}^{2\pi}\int_{-1}^{1} Y_n^m\, Y_j^{k*}\, d\mu\, d\lambda = \delta_{mk}\,\delta_{nj} \qquad (2.7.23)$$

CHAPTER THREE

NUMERICAL ALGORITHM

This chapter presents the salient features of the numerical algorithm used in the present work. The topics covered include the spectral representation of U, V, Ψ, and ζ fields, computation of the grid points, computation of the coefficients from the grid point values of the scalar fields and vice-versa, computation of the derivatives of the fields, the non-dimensionalization of the governing differential equations, and the spectral form of the governing differential equation. Back and forth transformation of Ψ and ζ fields, and computation of the Jacobian(non-linear terms) are also brought out in this chapter. The later part of the chapter includes the time-stepping scheme, the flow chart, a description of the types of scalar spectra used in the analysis.

(3.1) Spectral representation of scalar fields

In this section, we present the spectral expansions of the scalar quantities used in our study. We use the so-called rhomboidal type of truncation. These variables are the steam function(ψ), the vorticity (ζ), and the weighted x and y components of velocity (U and V respectively). The last two quantities are defined by

$$U \equiv u \cos\phi \ , \quad V \equiv v \cos\phi \tag{3.1.1}$$

where u, v are the components of the actual velocity, ϕ is the latitude. The velocity components are so redefined, because (U, V)

are more convenient to use in the spectral barotropic equation. The spectral representation of the U, V, ψ, and ζ fields are given below

$$U = \sum_{m=-N+1}^{N-1} \sum_{n=|m|}^{N+|m|} U_n^m \; Y_n^m \qquad (3.1.2)$$

$$V = \sum_{m=-N+1}^{N-1} \sum_{n=|m|}^{N+|m|} V_n^m \; Y_n^m \qquad (3.1.3)$$

$$\psi = \sum_{m=-N+1}^{N-1} \sum_{n=|m|}^{N+|m|-1} \psi_n^m \; Y_n^m \qquad (3.1.4)$$

$$\zeta = \sum_{m=-N+1}^{N-1} \sum_{n=|m|}^{N+|m|-1} \zeta_n^m \; Y_n^m \qquad (3.1.5)$$

where $Y_n^m = P_n^m(\mu)\, e^{im\lambda}$, the Spherical Harmonic functions, $\mu = \sin\phi$, and U_n^m, V_n^m etc are the spectral coefficients of the corresponding physical quantities. In the above equations N is the rhomboidal truncation number, and m and n are the 2-D wave numbers. The spectral coefficients are (complex) functions of time. The truncated series for U, V have one more term (in the n summation) than the series for ψ and ζ for the reasons that will become obvious later.

(3.2) The Grid -point representation

For a given truncation number N, some restrictions are imposed on the number of grid points used in the numerical model

in order to obtain alias-free computations. These restrictions are necessary for the non-aliased calculation of non-linear term (e.g.,Jacobian term) using the transform method. For rhomboidal truncation N , the number of grid points in the longitudinal direction must be greater or equal to 3N and in the latitudinal direction the number of grid points should be greater or equal to $\frac{5N + 1}{2}$. These limits are built into the subroutine for the grid-spectral transforms. Therefore for N=16, we choose a grid point representation of 48×40(the first number corresponds to the longitudinal direction and the second in the latitudinal direction).

(3.3) Computation of the grid points

For exact evaluation of a integral using Gaussian quadrature the grid points are chosen as zeros or the roots of an appropriate trial functions. In our problem (2-D on a sphere) the natural function to use are the spherical harmonics(eigen functions of *poissons* equation on a sphere). The spherical harmonics are the product of an associated Legendre polynomial and a Fourier term. Therefore the grid points in the zonal or longitudinal direction are equally spaced (as for a Discrete Fourier transform), and in the meridional direction grid points are selected as zeros of the K^{th} order Legendre polynomial (which are unevenly spaced) where K is the number of grid points in that direction.

(3.4) Computation of the coefficients from the grid points values and vice-versa

The spectral representation of a function $A(\lambda,\mu)$ is

$$A(\lambda_j,\mu_k) = \sum_{m=-N+1}^{N-1} \sum_{n=|m|}^{N+|m|-1} A_n^m \, P_n^m(\mu_k) \, e^{i m \lambda_j} \qquad (3.4.1)$$

defined on some suitable set of points λ_j, and μ_k.

The spectral coefficients A_n^m are calculated from $A(\lambda,\mu)$, using the orthogonality property of the trial functions :

$$A_n^m = \frac{1}{2\pi} \int_0^{2\pi} \int_{-1}^{1} A^m Y_n^* \, d\lambda \, d\mu \qquad (3.4.2)$$

where the starred quantity is a complex conjugate. Here the limit of integration for λ varies from 0 to 2π, and that for μ from -1 to 1. Generally the evaluation of the integral in (3.4.2) in carried out in two steps

$$A^m(\mu) = \frac{1}{2\pi} \int_0^{2\pi} A(\lambda,\mu) \, e^{-i m \lambda} \, d\lambda \qquad (3.4.3)$$

and

$$A_n^m = \int_{-1}^{1} A^m(\mu) \, P_n^m(\mu) \, d\mu \qquad (3.4.4)$$

As we have function values at only a finite set of grid points, we can not directly use the equations (3.4.3) and (3.4.4). Generally quadrature formulas (Gaussian, Trapezoidal, etc) are used to evaluate the above integrals. The equation (3.4.3) is calculated using a *trapezoidal* rule formula. Using this rule we can rewrite

equation (3.4.3) as

$$A^m(\mu_k) = \frac{1}{2 M \pi} \sum_{j=0}^{M-1} A(\lambda_j, \mu_k)\, \bar{e}^{im\lambda_j} \qquad (3.4.5)$$

where $\lambda_j = \frac{2\pi}{M} j$,and j denotes the position of the grid points in the longitudinal direction and M is the total number of grid points in the longitudinal direction and is equal to 3N. For any function which may be represented as a truncated Fourier series with wave number less than M, this formula is exact. Generally, Fast Fourier Transforms (*FFT*) are used to evaluate (3.4.5).

The *Gauss-Legendre quadrature* is used to evaluate equation (3.2.4). We can rewrite equation (3.2.4) using the Gaussian quadrature as

$$A_n^m = \sum_{k=1}^{K} W(\mu_k)\, A^m(\mu_k)\, P_n^m(\mu_k) \qquad (3.4.6)$$

The sum is carried out over the K latitudes μ_k, where μ_k are the roots of the ordinary Legendre polynomial of order K [ie. $P_K(\mu_k) = 0$] and are called *Gaussian latitudes*; $W(\mu_k)$ are the *Gaussian weights*. The Gaussian quadrature formula is exact for any polynomial of degree $\leq 2K - 1$. The number of Gaussian latitudes are chosen as K=5M/2. It is clear that equation (3.4.6) is a multiplication involving a weight function matrix[with elements $W(\mu_k)$], a coefficient matrix[with elements $A^m(\mu_k)$], and an associated Legendre polynomial matrix[with elements $P_n^m(\mu_k)$]. We have already explained the method of the computing weight function matrix in the chapter 2. We will later explain the computation of the associated Legendre polynomial matrix or *P* matrix.

We can also compute the grid point values, if the spectral coefficients A_n^m are known, by evaluating equation (3.4.1). Again this computation is performed in two steps. In the first step, we calculate $A^m(\mu_k)$ using the relation given below

$$A^m(\mu_k) = \sum_{n=|m|}^{N+|m|-1} A_n^m \; P_n^m(\mu_k) \qquad (3.4.7)$$

Equation (3.4.7) is basically a multiplication of a coefficient matrix and an associated Legendre polynomial matrix. The second step uses a transform method or FFT to find the grid point value of the function $A(\lambda_j,\mu_k)$. The equation used is given below

$$A(\lambda_j,\mu_k) = \sum_{m=-N+1}^{N-1} A^m(\mu_k) \; e^{i\,m\,\lambda_j} \qquad (3.4.8)$$

The transformation from the grid or the physical space to the spectral space is called the *Forward* transform whereas that from the spectral space to the grid space is called *Backward* or *inverse* transform. Generally, we call equation (3.4.5)-(3.4.6) as forward transform pair and equation (3.4.7)-(3.4.8) as backward transform pair.

(3.5) Computation of the meridional and the zonal derivatives

The reasons spectral methods have gained increasing popularity in applications requiring numerical solution of PDE's is that they allow extremely accurate evaluation of derivatives.

Calculation of the zonal derivatives

Consider once again the spectral expansion

$$A(\lambda,\mu) = \sum_m \sum_n A_n^m \, P_n^m(\mu) \, e^{im\lambda} \qquad (3.5.1)$$

By differentiating (3.5.1) with respect to λ, we get

$$\frac{\partial A(\lambda,\mu)}{\partial \lambda} = \sum_m \sum_n A_n^m \, P_n^m(\mu) \quad (im) \quad e^{im\lambda}$$

$$= \sum_m \sum_n D_n^m \quad P_n^m(\mu) \quad e^{im\lambda} \qquad (3.5.2)$$

where $D_n^m = i\,m\,A_n^m$. From (3.5.1, 3.5.2) it is clear that the spectral coefficients of the derivative (D_n^m) in the zonal direction are related to the original coefficients (A_n^m) by a very simple relation. Once D_n^m is found out the transform pair method [as in (3.4.7)-(3.4.8)] are used to calculate the values of the zonal derivatives at grid points.

Computation of the meridional derivative

By differentiating (3.5.1) with respect to μ , we get

$$\frac{\partial A(\lambda,\mu)}{\partial \mu} = \sum_m \sum_n A_n^m \, \frac{\partial P_n^m(\mu)}{\partial \mu} \, e^{im\lambda} \qquad (3.5.3)$$

The derivative of an associated Legendre polynomial in (3.5.3) is calculated using the recursive relationships. Once we know this derivative matrix, with element $DP_n^m(\mu_k) \equiv \frac{\partial \, P_n^m \mu_{\,k}}{\partial \, \mu}$, the transform

pair (3.4.7)-(3.4.8) is used to calculate the grid point values of the meridional derivative of a given function. The computation of this derivative matrix or *DP* matrix of associated Legendre polynomial is explained in the next section.

(3.6) Computation of Associated Legendre Polynomial and its Derivative

The associated Legendre polynomial are a family of orthogonal polynomials in the interval (-1, 1) and have a weight function w = 1.

The associated legendre polynomials of the first kind normalized to unity are represented by

$$P_n^m(\mu)=\left\{\frac{(2n+1)\ (n-m)!}{2\qquad (n+m)!}\right\}^{1/2}\frac{(1-\mu^2)^{m/2}}{2^n\ n!}\frac{d^{m+n}}{d\mu^{m+n}}\ (\mu^2-1)^n \qquad (3.6.1)$$

Associated Legendre polynomial (normalized one) satisfy the orthogonal relationship given below

$$\int_{-1}^{1} P_n^m\ \ P_k^m\ \ d\mu = \delta_{nk} \qquad (3.6.2)$$

The P_n^m rapidly become cumbersome to represent - the first few functions are

$$P_0^0 = \sqrt{1/2}$$

$$P_1^0 = \sqrt{3/2}\ \mu$$

$$P_2^0 = \sqrt{5/2}\ (1/2)\ (3\ \mu^2 - 1) \quad \text{etc.}$$

It is clear from the above expressions that it will be better if we use some other means to generate the associated Legendre polynomials in a numerical model. Generally the P_n^m or P matrix are all obtained using the following relationships

$$P_n^m = 0 \quad , n < m \tag{3.6.3}$$

$$P_n^{-m} = (-1)^m\ P_n^m \tag{3.6.4}$$

and the recursion relations

$$P_{n+1}^n = \sqrt{2n+3}\ \mu\ P_n^m \tag{3.6.5}$$

$$\varepsilon_{n+1}^m\ P_{n+1}^m = \mu\ P_n^m - \varepsilon_n^m\ P_{n-1}^m \tag{3.6.6}$$

$$P_{n+1}^{n+1} = \left[\frac{2n+3}{2n+2}\right]^{1/2} \left[1 - \mu^2\right]^{1/2} P_n^n \tag{3.6.7}$$

where

$$\varepsilon_n = \left[\frac{n^2 - m^2}{4n^2 - 1}\right]^{1/2} \tag{3.6.8}$$

The elements of the P matrix used in the forward-backward transform are defined as $P(m, n, \mu_i) \equiv P_n^m(\mu_i)$. The way this matrix is generated is as follows: For any given μ_k, $P_0^0(\mu_k)$ is $\sqrt{1/2}$, then P_1^0 is computed using (3.6.5), and the higher n values for n=0 can be computed using (3.6.6) and the previously computed values of P. Then (3.6.7) can be used to generate $P_1^1(\mu_k)$ and the process repeated using (3.6.5) and (3.6.6). Similarly the P values at the m=2, 3, 4..... levels can be generated. For the next μ_k the entire process will have to be repeated.

Once we know the all $p_n^m(\mu_k)$'s, the derivatives of associated Legendre polynomials or *DP* matrix are calculated using the relation

$$(1-\mu^2)\frac{dP_n^m}{d\mu} = -n\,\varepsilon_{n+1}^m P_{n+1}^m + (n+1)\,\varepsilon_n^m P_{n-1}^m \qquad (3.6.9)$$

where $\frac{dP_n^m}{d\mu}$ at μ is the element of the derivative matrix *DP*(m, n, μ_k).

In this way we can generate P and DP matrix .These matrix are used in *backward* and *forward* transformation and in computing the meridional derivatives of the dependent variables.

(3.7) Non-dimensionalization of the governing equation

The problem under consideration in the present work is that of the non-divergent barotropic vorticity equation. The corresponding governing equation in spherical form is given below

$$\frac{\partial\zeta}{\partial\tau} = -\frac{1}{a\cos^2\phi}\left[\frac{\partial}{\partial\lambda}\left[U\,\zeta\right] + \cos\phi\frac{\partial}{\partial\phi}\left[V\,\zeta\right]\right] - 2\,\Omega\frac{V}{a} \qquad (3.7.1)$$

where

$$U = -\frac{\cos\phi}{a}\frac{\partial\psi}{\partial\phi} \qquad (3.7.2)$$

$$V = \frac{1}{a}\frac{\partial\psi}{\partial\lambda}\,, \qquad (3.7.3)$$

$$\zeta = - \frac{\partial U}{\partial \mu} + \frac{1}{\cos^2\phi} \frac{\partial V}{\partial \lambda} \qquad (3.7.4)$$

Here a is the mean radius of earth and Ω is the rotation rate of the earth. The primary directions are: longitude λ increasing to the east, latitude ϕ increasing to the north.

For convenience equation (3.7.1) is changed to non-dimensional form by using radius of the earth as length scale and $(2\ \Omega)^{-1}$ as the time scale, as in Washington and Parkinson[18]. The quantities with * as superscript are non-dimensional quantities.

$$t^* = 2\ \Omega\ t \quad , \quad x^* = \frac{x}{a} \quad ,$$

$$U^* = \frac{U}{2\ \Omega\ a} \quad , \quad V^* = \frac{V}{2\ \Omega\ a} \quad ,$$

$$\psi^* = \frac{\psi}{2\ \Omega\ a^2} \quad ,$$

$$\zeta^* = \frac{\zeta}{2\ \Omega}$$

Substitution in (3.7.1) gives

$$\frac{\partial \zeta^*}{\partial t^*} = - \frac{1}{\cos^2\phi} \left[\frac{\partial}{\partial \lambda} (U^*\ \zeta^*) + \cos\phi \frac{\partial}{\partial \phi} (V^* \zeta^*) \right] - V^* \qquad (3.7.5)$$

We can write U^* and V^* in terms of the derivatives of non-dimensional stream function :

As $$U = - \frac{\cos\phi}{a} \frac{\partial\psi}{\partial\phi}$$

therefore,

$$U^* \; 2 \; \Omega \; a = - \frac{\cos\phi}{a} \; 2 \; \Omega \; a^2 \; \frac{\partial\psi^*}{\partial\phi}$$

which becomes

$$U^* = - \cos\phi \; \frac{\partial\psi^*}{\partial\phi}$$

and finally,

$$U^* = - \cos^2\phi \; \frac{\partial\psi^*}{\partial\mu} \qquad \left[\text{using } \frac{\partial}{\partial\phi} = \frac{\partial\mu}{\partial\phi} \frac{\partial}{\partial\mu} = \cos\phi \frac{\partial}{\partial\mu}\right]$$

while

$$V = \frac{1}{a} \frac{\partial\mu}{\partial\lambda}$$

becomes $$V^* = \frac{\partial\psi^*}{\partial\lambda}$$

substituting U^*, V^* ,and $\frac{\partial}{\partial\phi} = \cos\phi \frac{\partial}{\partial\mu}$ in (3.1.5), we get

$$\frac{\partial\zeta^*}{\partial t^*} = - \left[- \frac{\partial}{\partial\lambda} \left(\frac{\partial\psi^*}{\partial\mu} \zeta^* \right) + \frac{\partial}{\partial\mu} \left(\frac{\partial\psi^*}{\partial\lambda} \zeta^* \right) \right] - \frac{\partial\psi^*}{\partial\lambda}$$

Dropping * for convenience, we can write above equation as

$$\frac{\partial\zeta}{\partial t} = - \left[- \frac{\partial}{\partial\lambda} \left(\frac{\partial\psi}{\partial\mu} \zeta \right) + \frac{\partial}{\partial\mu} \left(\frac{\partial\psi}{\partial\lambda} \zeta \right) \right] - \frac{\partial\psi}{\partial\lambda}$$

$$\frac{\partial\zeta}{\partial t} = - \left[- \frac{\partial}{\partial\lambda} (\psi_\mu \zeta) + \frac{\partial}{\partial\mu} (\psi_\lambda \zeta) \right] - \psi_\lambda$$

On simplification, the term inside the bracket can be rewritten as

$$\frac{\partial \zeta}{\partial t} = \left[\psi_\mu \zeta_\lambda - \psi_\lambda \zeta_\mu \right] - \psi_\lambda \qquad (3.7.6)$$

The term inside the bracket is called the Jacobian which is basically consists of the non-linear terms.

(3.8) Governing equation in the Spectral form

We now present the spectral form of the non-dimensional non-divergent barotropic vorticity equation used in the present study.

We have already derived the non-dimensional form of the governing equation (3.7.6), and discussed the spectral representations of the scalar fields. We write the non-dimensional barotropic vorticity equation in the spectral form as

$$\frac{\partial \zeta_n^m}{\partial t} = F_n^m - i\, m\, \psi_n^m , \quad \begin{matrix} 0 \le m \le N-1 \\ m \le n \le m + N - 1 \end{matrix} \qquad (3.8.1)$$

where ζ_n^m and ψ_n^m are the complex coefficients of vorticity and stream function, respectively. The coefficients F_n^m are the spectral coefficients of the Jacobian [$\equiv (\psi_\mu \zeta_\lambda - \psi_\lambda \zeta_\mu)$]. Note that equation (3.8.1) need not be evaluated for negative m. This is because we are dealing with real fields and this property can be used in finding, say, ζ_n^{-m} from ζ_n^m by using

$$\zeta_n^{-m} = (-1)^m \zeta_n^{m*} \qquad (3.8.2).$$

(3.9) Computation of ψ coefficients from ζ coefficients and vice-versa

The stream function ψ is related to vorticity ζ by relation

$$\zeta = \nabla^2 \psi \qquad (3.9.1$$

where ζ, ψ, and the laplacian operator are al non-dimensionalized. Now

$$\nabla^2 Y_n^m = -n\,(n+1)\, Y_n^m \qquad (3.9.2$$

Considering (3.9.1) and (3.9.2) along with the spectra representations of ψ and ζ [(3.1.4) and (3.1.5)] we see that th spectral coefficients of ψ and ζ are related by

$$\zeta_n^m = -n\,(n+1)\, \psi_n^m \qquad (3.9.2)$$

So given either ψ_n^m or ζ_n^m we can compute the other by multiplyin or dividing by $-n\,(n+1)$, respectively.

(3.10) Computation of the Jacobian

The Jacobian comprises of the product of longitudinal an meridional derivatives of ζ and ψ) :

$$J(\zeta,\psi) = (\psi_\mu\, \zeta_\lambda - \psi_\lambda\, \zeta_\mu) \quad . \qquad (3.10.1)$$

The pseudo-spectral technique is used to evaluate this term. That is, given the spectral coefficients of ψ and ζ, we first compute the grid point values of the longitudinal and meridional derivatives of these functions by using the techniques presented in section (3.5). The grid point values of the Jacobian are then evaluated from (3.10.1). The grid point values are then transformed to obtain the spectral coefficients of the Jacobian i.e. F_n^m. This method is called pseudo-spectral bacause the multiplications are not done in spectral space but rather in physical (grid) space.

(3.11) Flow-chart

A flow chart given in Fig.(A) summarizes the algorithm used in the present work. We used pseudo-spectral technique in our problem (i.e., all multiplications have been performed on physical space or at grid points and all derivative calculations have been performed on spectral space). The time stepping scheme used is finite difference leap-frog scheme with a forward-difference start.

(3.12) The spectrum of a scalar field

One very important analytic tool is the study of unsteady velocity fields concerns the distribution of energy at the various length scales in the problem. The usual method for obtaining this information is to construct spectra of energy versus the wave number. These spectra can be three, two or one dimensional. In isotropic fluids, generally, one dimensional spectra are preferred because of convenience in plotting. In spherical coordinates two

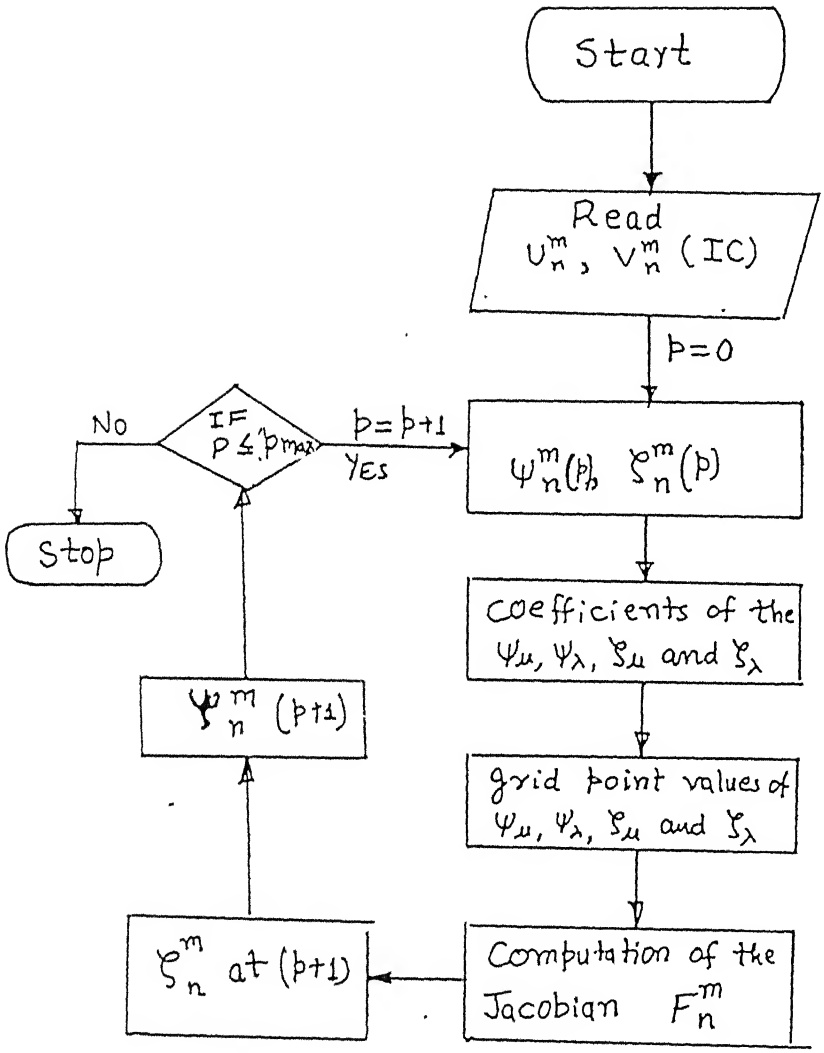

p = time-step

FLOW-CHART

types of one-dimensional spectra are defined namely the so-calle "m" spectrum which depicts the energy distribution in the 'm' wav number of the coefficients A_n^m and the "n" spectrum, which does th same for the 'n' wave number.

The spectrums:

Let H be a scalar field. We can write global average of H as

$$\langle H \rangle = \frac{1}{4\pi} \int_0^{2\pi} \int_{-1}^{1} H \, d\mu \, d\lambda \qquad (3.12.1$$

As $H = \sum_m \sum_n H_n^m Y_n^m$, the equation (3.12.1) becomes

$$= \frac{1}{4\pi} \sum_m \sum_n \int_0^{2\pi} \int_{-1}^{1} H_n^m Y_n^m \, d\mu \, d\lambda$$

$$= \frac{1}{4\pi} \sum_m \sum_n H_n^m \int_0^{2\pi} \int_{-1}^{1} Y_n^m \, d\mu \, d\lambda$$

These integrals are zero for all m, n except m=0 and n=0.

$$\therefore \quad \langle H \rangle = \frac{H_0^0}{\sqrt{2}} \qquad (3.12.2$$

We can also derive the expression for ensemble average of square of any scalar field H. We write

$$\langle H^2 \rangle = \frac{1}{4\pi} \int_0^{2\pi} \int_{-1}^{1} H H^* \, d\mu \, d\lambda$$

$$= \frac{1}{4\pi} \sum_n \sum_m \sum_p \sum_q \int_0^{2\pi} \int_{-1}^{1} H_n^m H_q^{p*} Y_n^m Y_n^{p*} \, d\mu \, d\lambda$$

Using the orthogonality relationship we can rewrite this as

$$\langle H^2 \rangle = \frac{1}{4\pi} \sum_n \sum_m \sum_p \sum_q H_n^m \; H_q^{p*} \; \delta_{mp} \; \delta_{nq}$$

$$= \sum_n \sum_m \frac{H_n \; H_n}{2} \qquad (3.12.3$$

where * indicates a complex conjugate.

The fluctuating part of the scalar quantity is

$$H^{\#} = H - \langle H \rangle \quad .$$

$$\therefore \langle H^{\#2} \rangle = \langle H^2 \rangle - \langle H \rangle^2$$

Substituting (3.12.2) and(3.12.3) in the above expression, we get

$$\therefore \langle H^{\#2} \rangle = \sum_m \sum_n \frac{H_n^m \; H_n^{m*}}{2} - (H_o^o / 2)$$

$$\therefore \langle H^{\#2} \rangle = \sum_m \sum_n \frac{H_n^m \; H_n^{m*}}{2} \qquad (m=n\neq 0) \qquad (3.12.4.$$

The variance (or 'energy') of the field is thus decomposed into its 'energy' at individual wave numbers.This allows the calculation of a 2-D spectrum E_n^m.

$$E_n^m \equiv \begin{cases} H_n^m \; H_n^{m*} & \text{for } m > 0 \quad n \geq |m| \\ (H_n^m \; H_n^{m*})/\,2 & \text{for } m = 0 \quad n \geq 0 \end{cases}$$

Now as E_n^m is the same as E_n^{-m} for real fluids so we can sum over all non-negative m to get

$$\langle H^{\#2} \rangle = \sum_{m=0}^{N-1} \sum_{n=|m|}^{|m|+N-1} E_n^m \qquad (m=n=\neq 0 \text{ excluded}) \qquad (3.12.5)$$

Similarly we can define the one dimensional 'm'spectrum F(m) such that

$$\langle H^{\#2} \rangle = \sum_{m=0}^{N-1} F(m) \qquad (3.12.6)$$

where
$$F(m) = \begin{cases} \sum_{m=1}^{N-1} E_n^0 & , \quad m = 0 \\ \sum_{n=|m|}^{|m|+N-1} E_n^m & , \quad m \geq 1 \end{cases} \qquad (3.12.7)$$

We can also define the "n" spectrum G(n) such that

or
$$\langle H^{\#2} \rangle = \sum_{n=0}^{2N-2} G(n) \qquad (3.12.8)$$

where
$$G(n) = \begin{cases} 0 & , n=0 \\ \frac{|H_n^0|}{2} + \sum_{m=1}^{N-1} |H_n^m|^2 & , 1 \leq n \leq N-1 \\ \sum_{m=n-N+1}^{N-1} |H_n^m|^2 & , N-1 \leq n \leq 2(N-1) \end{cases} \qquad (3.12.9)$$

The equations (3.12.7) and (3.12.9) are used to evaluate the spectra of of U, V, and ζ fields. The importance of m and n spectra lies in the fact that they gives us a good idea of the relative distribution of energy in the wave number space.

CHAPTER 4

RESULTS AND DISCUSSIONS

In this chapter, we present results that demonstrate the effect of truncation of IC on the error growth, a comparison of resolution error and the initial condition dependent error (ICD), and a study of the relative rates of increase of the low wave number and the high wave number errors.

Initial condition, in the form of say 42×41 spectral coefficients (per level) of u, v, P etc, are commonly obtained from objective analysis. Most of the energy in these fields is in the low wave number coefficients. We seek to study the effect of "truncation" of these spectral coefficients on the growth rate of error. Truncation is the procedure by which only the spectral coefficients corresponding to a Rhomboidal truncation number N are used and the others are discarded. For example if we truncate the IC at N=16, we will use only the lowest order 256 of the available 42×41 coefficients.

The truncation of IC causes the loss of information contained in the high wave number coefficients and hence introduces an initial error. We truncate the "exact" IC at the rhomboidal truncation number N =16, and 32, to study the growth of error for the above two cases. The computations are performed on 192×160 grid(corresponding to N=64 calculation). The vorticity field is found to be more sensitive to the truncation of IC compared to the velocity fields as there energy is distributed over a wide wave number range compared to the velocity fields which have there most of the energy in the low wave numbers only.

The CPU time increases very rapidly with an increase in the resolution. As we know that our initial condition is most likely to be inaccurate in spite of our best effort, therefore there is a no point in increasing resolution beyond the point where initial condition dependent error (ICD) becomes dominant. A comparison of the growth of the resolution error and the initial condition dependent error(ICD) gives an insight into this problem. As our study shows that if the IC contains 10% error (Standard deviation=0.1), then it is not advisable to perform the computations on the 192×160 (N=64) grid because the computations on the 96×80 (N=32) grid also gives adequate resolution in simulation upto a period of three-days. To study the resolution error effect, we consider three sets of grids 192×160 (N=64), 96×80 (N=32), and 48×40 (N=16). To study the ICD error, we artificially introduce errors (5% ,and 10% rms error) on "exact" IC and then simulate it for 3-days on 192×160 grid.

A comparison of the rms error growth due to the errors in the low wave number coefficients and that in the high wave number coefficients shows that in the first case rate of error growth is faster than that in the second case.The sensitivity of the solution to the distribution of error(or random number sets) is also carried out in the present study. The result shows that, although quantitatively there are slight variations, qualitatively the conclusions remains same. The method of perturbing the high wave number as well as the low wave number coefficients is explained later in this chapter.

(4.1) Generation of Standard Initial Condition

In this section, we present the method for generating the initial conditions for our problem. Our initial data was obtained

from objectively analyzed conditions for Feb 19, 1990 and was obtained from the NCMRWF, New Delhi. It contains 42×41 spectral coefficients per level for the u, and v fields. We used the 500 mb level data for generating our initial conditions. Therefore we calculate the initial vorticity coefficients from these initial u and v coefficients. We use only 256 u, v coefficients corresponding to rhomboidal truncation number 16; these makeup about 95% of the total available energy in 500 mb velocity field. The reason for neglecting the higher modes of u, and v is that they will introduce unnecessary noise while calculating ζ coefficients from the u and v coefficients. This is because the vorticity depends on the differentials of the velocity components and the process of differentiation magnifies the importance of the the high wave wave number coefficients. Therefore the 256 u, v coefficients are used to determine the grid point values (on a 48×40 grid) of U and V, and then of the meridional and zonal derivatives of U and V respectively. The grid point values of the vorticity are then computed using equation (3.7.4). These grid point values are then transformed to obtain the 256 vorticity coefficients.

The ζ spectrum obtained with only 256 spectral coefficients is unphysical because it drops to zero after truncation wave number N=16. Therefore we artificially generate energy in the higher modes in the following manner: the 256 coefficients of ζ are used as initial condition and we run the program for 5-days on 192×160 (N=64)grid. This gives us a smooth spectrum of vorticity. Also, as five days is the order of the large time-scales of the atmosphere we can expect that the high wave number regions of the spectrum to have reached an equilibrium by this time. This ensures that the spectrum obtained is physically valid in the higher wave numbers. If we had used 4096 coefficients of u, v to generate 4096 coefficients of ζ, we would have obtained noisy unphysical coefficients in the higher wave numbers. In this way, we generated

4096 coefficients of ζ, which we will refer as the "exact" initial condition or the standard initial condition in the coming sections.

It may be recalled, that for alias free computation the number of grid points should be 3N and 5N/ 2, in the longitudinal and meridional direction, respectively. So an N=64 computation can be done on a grid of 192x160 where the first number gives the number of grid points in the longitudinal direction and the second number in the meridional direction.

Fig (1a) presents plots of m spectrum of our initial U, V, ζ fields with N=64. Fig(1b) shows the m-spectrum of U on a Log-Linear scale at t=0 and t=3 days.

(4.2) Method of measuring errors

The error in computation (or prediction) of individual coefficients may occur either due to the propagation of error (like lack of observational data, inaccurate data etc.) in the initial data or due to bad resolution in the computation.

To study the effect of the initial condition dependent (ICD) error on the accuracy of the prediction, we perturb the standard initial condition by a known amount; while the effect of resolution on the loss of predictability is studied using three different sets of grids e.g., 48 × 40, 96 × 80, and 192 × 160(corresponding to N=16, 32, and 64, respectively). For both cases, the error in the prediction of individual coefficient is calculated by defining

$$\chi_n^m \equiv (\eta_n^m - \xi_n^m) \qquad (4.2.1)$$

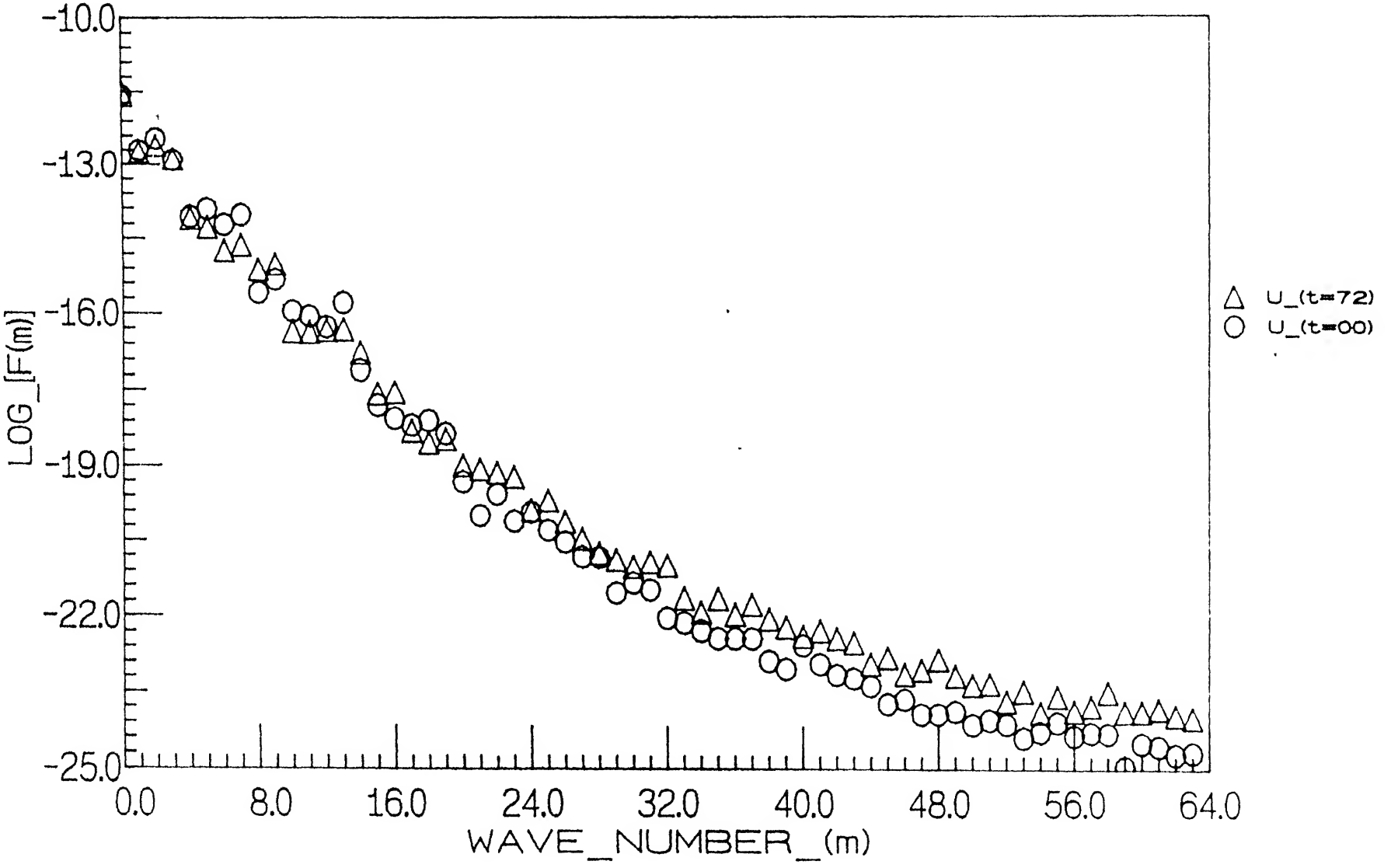

FIG.(1b) SPECTRA_OF_IC(U_VEL)

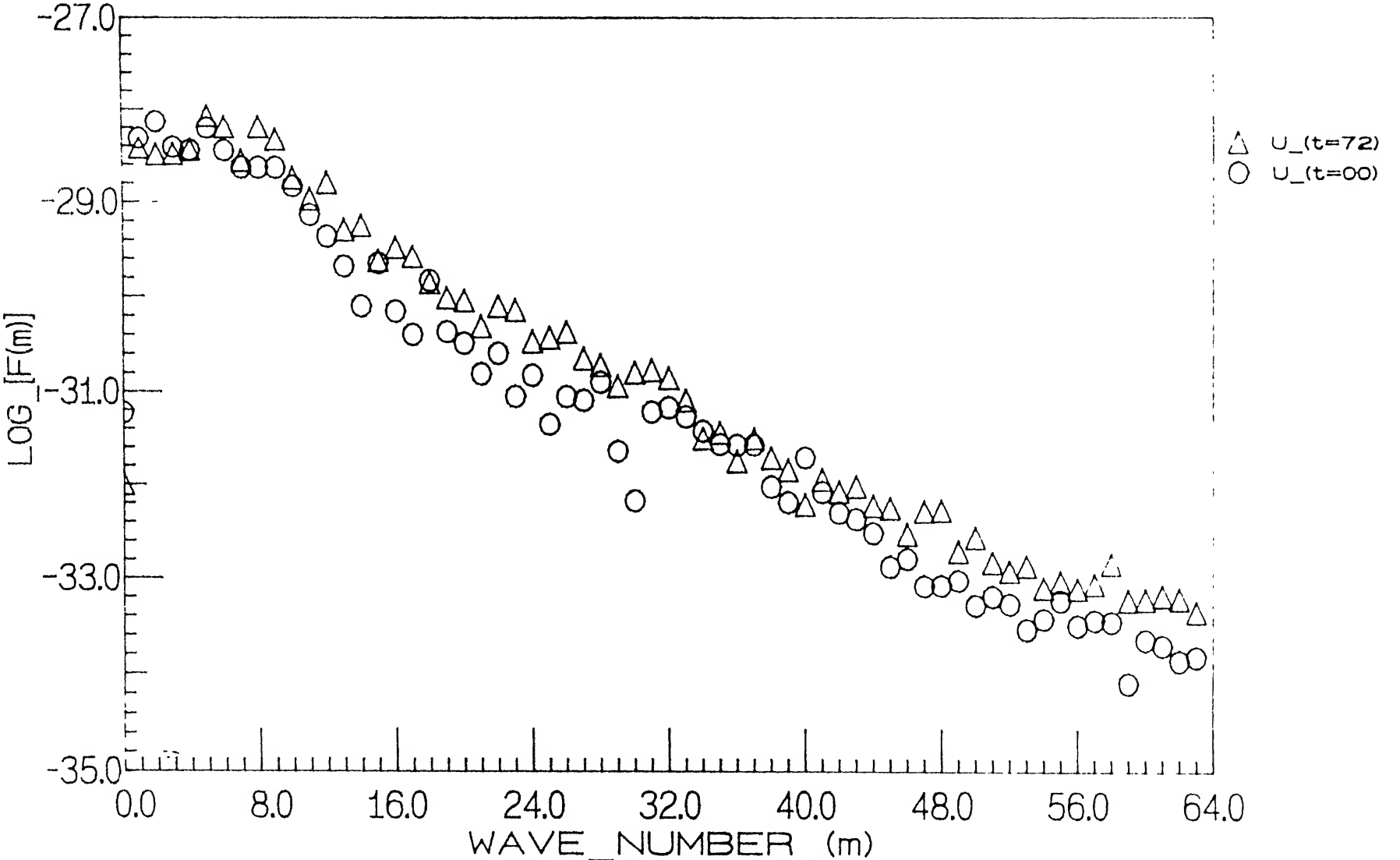

FIG.(1c) RESOLUTION_ERROR_SPECTRA(U_VEL)

where η_n^m is a coefficient obtained from the perturbed initial data or on the coarser grid and ξ_n^m is a coefficient corresponding to the exact solution obtained on the highest resolution and with the "exact" initial condition. Having computed the error coefficients χ_n^m for all (m,n) we can compute the 'error' spectrum in the usual way described in the last chapter.

Now the *error variance* is defined as

$$\langle H^{\#2} \rangle \equiv \sum_{n,m} (\eta_n^m - \xi_n^m)^2 \qquad (4.2.2)$$

where η and ξ are the physical space variables whose coefficients are η_n^m and ξ_n^m ; the brackets $\langle\ \rangle$ indicate a space average. The error spectrum is related to the error variance in the manner shown in equation(3.12.5) in the last chapter. Fig(1c) shows the 'm' spectrum of error in U at t=0 and t=3 days for N=32 computations. The error shown is the resolution error compared with the 'exact' (N=64) computation.

Another measure of error used in the present study is a RMS (root mean square) error of the coefficients. The formula for calculation of RMS error is given below

$$r \equiv \sqrt{\sum (\eta_n^m - \xi_n^m)^2 \quad / \sum \langle \xi_n^m \rangle^2} \qquad (4.2.3)$$

where r is a RMS error, and summations are done over all m, n.

(4.3) Sensitivity to truncation of initial condition

In this section, we investigate sensitivity of the simulations to truncation of the initial condition. Our so called exact initial condition contain 4096 spectral coefficients of ζ (corresponding to N=64). We consider here two cases (i.e.

truncation number N = 16 and 32) to study the effect of truncation of initial condition on the evolution of the model atmosphere. The computation performed using all the coefficients of our standard initial condition is used as a basis for comparison. Note that all the above computation are perrormed on 192×160 grid. Thus, the resolution in all the simulations will be the same: the only difference being in the initial condition error introduced by the truncation.

In the first case, we use only inner 256 coefficients (corresponding to N =16) of our exact initial condition, but keep all the other parameters same. The 192×160 simulation has 4096 spectral coefficients. Thus zero values are assigned to all the coefficients other than inner 256 coefficients of our so called exact initial condition. The computations are done for 3-days using this truncated initial condition. This simulation is compared with the "exact" simulation on the same grid using the full 4096 coefficients of the "exact" initial condition. The method of computing error spectrum and RMS value is already discussed in section (4.2).

Similarly we repeat the above steps for the second case (N=32). The initial condition for this case is obtained by assigning zero values to all the coefficients other than inner 1024 coefficients (corresponding to N=32) of exact initial condition

Fig (2) present plots between RMS value and time for both cases. In the Fig(2) following notations are used :

- (U/256), and (V/256) shows the results for U, and V fields using only 256 spectral coefficients of "exact" IC.
- (U/1024), and (V/1024) shows the results for U, and V fields using only 1024 spectral coefficients of "exact" IC.

The RMS error for the U field due to the truncation of IC is 17.2% and 5.2% for the two cases N=16, and 32, and for the V field it is 15.8% and 3.7% respectively. The corresponding figures for the vorticity is much higher, being 48.3% and 25.2%, respectively. The low RMS error for the U, and V fields compared to ζ field can be understood from the fact that the U, and V fields have their most of energies in the low wave number range.

It is also clear from the Fig(2) that the RMS error curves are almost flat or they increase only slowly with respect to time. These result suggests that while truncation of initial condition (IC) introduces error in the computation, this error grows quite slowly with respect to time if sufficiently high resolution is used.

(4.4) Comparison of Resolution error vs ICD Error

In this section, a comparison is made between the growth of initial condition dependent(ICD) error and resolution error. The ICD error is studied by deliberately introducing error of known RMS in our so called exact initial condition. We consider the 5% and 10% (RMS) error case for this. We consider three different sets of grid (i.e. 48×40, 96×80,192×160) corresponding to N=16, 32 and 64, respectively, to study the resolution effect on growth of RMS error.

Initial condition dependent (ICD) error is studied by deliberately introducing error on standard initial conditions. This error is introduced by randomly perturbing the coefficients of the "exact" initial condition so as to cause an error of a specified standard deviation from the original coefficients i.e.

$$\eta_n^m = \zeta_n^m (1 + \rho) \qquad (4.4.1)$$

where ρ is a pseudo random number of uniform distribution with zero mean and specified SD(standard deviation), η_n^m is a new initial spectral coefficient with a perturbation about standard initial data, and ζ_n^m is a coefficient of the standard initial condition of vorticity. We consider here two cases corresponding to SD(standard-deviation)= 0.05 and 0.10. This corresponds to the initial condition containing 5% rms error, and 10% rms error, respectively. We perform calculations on the 192×160 grid.

Next we consider computations of resolution error. A study of this demonstrate the effect of grid-size on the accuracy of the solution of a given problem. As the number of grid-points is increased the accuracy of the solution increases, but the computing time increases very rapidly. Therefore an optimum selection of the grid which gives good accuracy with reasonable amounts of computation is very necessary. In these simulations, we consider computation on 192×160 grid as the "exact" one in comparison with simulations on coarser grid. This simulations can be used to compare the results obtained from computation on 48×40 and 96×80 grids. The initial condition for 48×40 grid requires 256 spectral coefficients, 1024 coefficients are required for computations on 96×80 grid and 4096 coefficients are required for 192×160 grid. These coefficients are selected from standard initial data by truncation. The RMS value is calculated using (4.2.3). It is clear that even in the beginning of the simulation the RMS error for the truncated IC will not be zero. For example, in the 256 coefficient IC problem η_n^m and ξ_n^m will be exactly same for the inner 256 coefficients but outside this region η_n^m will be zero while ξ_n^m will not be so. Thus the error will not be zero for all wave numbers and the RMS error will also be non-zero.

It is clear that, when the grid is made coarser, the IC also become truncated because a coarser grid can support less number of spectral coefficients. A question that immediately springs to mind is this : How important are the spectral coefficients that are discarded by truncation ? There are two aspects to the answer to this question. Firstly, it is true that the energy contained in the various wave numbers decrease dramatically with increase in the wave number. Therefore unless the truncation is at very low wave number (m<16), we would expect that the discarded coefficients to be of less importance than the retained ones. Secondly, we know that the higher order initial coefficients are more difficult to measure, because of various factors, and are therefore prone to be erroneous. Therefore when the higher order coefficients are discarded, not all of the loss will be *real* information. Therefore the 'worst case' for truncated IC will be when all the discarded coefficients are 'exact' (which is highly unlikely for real IC) and the 'best case' will be when they are all erroneous.

In keeping with the above arguments, we consider two cases in the resolution studies : The 'Worst' case scenario when all the 4096 coefficients of the IC are exact. Thus every discarded mode contributes real loss of information. In this case the N=16 and 32 simulations are compared with the N=64 computations with the 4096 coefficients of IC. In the 'Best' case scenario we regard only the first 400 coefficients (corresponding to N=20) to be exact and all the rest to be completely erroneous. This assumption, though idealized, is closer to the situation in real IC. In this case the N=16 and 32 computations are compared to the N=64 computation with a 400 coefficient IC. There will be a truncation of IC, it may be noted only in the N=16 case (because the N=32 computation has 1024 coefficients while the IC has only 400). This case is called "best case" because even the coarse grids in our study will capture most of the IC information as non-capturable large wave number range

have no energy.

The results of the ICD and the resolution error studies are shown in fig (3a)-(3c), where the RMS error in U, V and ζ, respectively, are shown versus time.The following notations are used :

- N=16/(W) and N=16/(B) shows the results for the computations on the 48×40 grid for the so called "worst" case and the "best" case respectively.
- N=32/(W) and N=32/(B) shows the results for the computations on the 92×80 grid for the so called "worst" case and the "best" case respectively.
- N=64/0.05(W) and N=64/0.05(B) shows the results for the computations on the 192×160 grid when the IC contains 5% rms error for the so called "worst" case and the "best" case respectively.
- N=64/0.10(W) and N=64/0.10(B) shows the results for the computations on the 192×160 grid when the IC contains 10% rms error for the so called "worst" case and the "best" case respectively.

From Fig(3a) and fig(3b) it is clear that the resolution error in U and V for the N=16 computation begins with an error 12-18% .This error is larger than we would typically expect to be in the initial conditions. Also the initial error increases quite rapidly, reaching to 25-30% in three days. Therefore, the N=16 computations offer degraded predictions both from the point of view of initial condition error (due to truncation) and also due to poor resolution. However, when we observe the RMS values for the N=32 simulations we see that the error level are lower than that in the simulation with 10% initial error for atleast three days even in the worst case. Indeed, for the best case scenario, the resolution errors in a N=32 calculations are below the ICD error for simulation beginning with 5% IC error for a period of

atleast three days. This suggests that given initial IC error of 5-10%, which is what we would expect in real objectively analyzed data, N=32 provides about the optimum resolution required for predictions of upto three days.

However, these conclusions hold only for the velocity field and not for the vorticity as figure(3c) shows. It can be seen that even N=32 gives unacceptably high initial errors of 25% (worst case) and 10% (Best case). This of course, is because the vorticity is very dependent on the small scale high wave number structure of the flow field and consequently contain much more energy in the higher wave number than does velocity field. This make is particularly sensitive to truncation which removes energy at the high wave numbers.

This suggests that given about 10% error level in the initial conditions we can perform simulations on an N=32 grid (92×80) rather than wasting computer time to do the same simulation on a finer grid.

Fig(3d)-(3f) shows the sensitivity of the IC error to random number sets (a) and (b). It can also be observed from the figures that the curves for the different random number sets are qualitatively similar. Therefore, above stated conclusions are independent of random sets used.

(4.5) Low wave number vs High wave number errors

In this section we investigate the wave-number dependence of the error growth. That is, first we introduce error only in the high wave number coefficients of the initial condition and then only in the low wave number coefficients and compare the growth of error in the two cases.Here we define 'Low wave number'

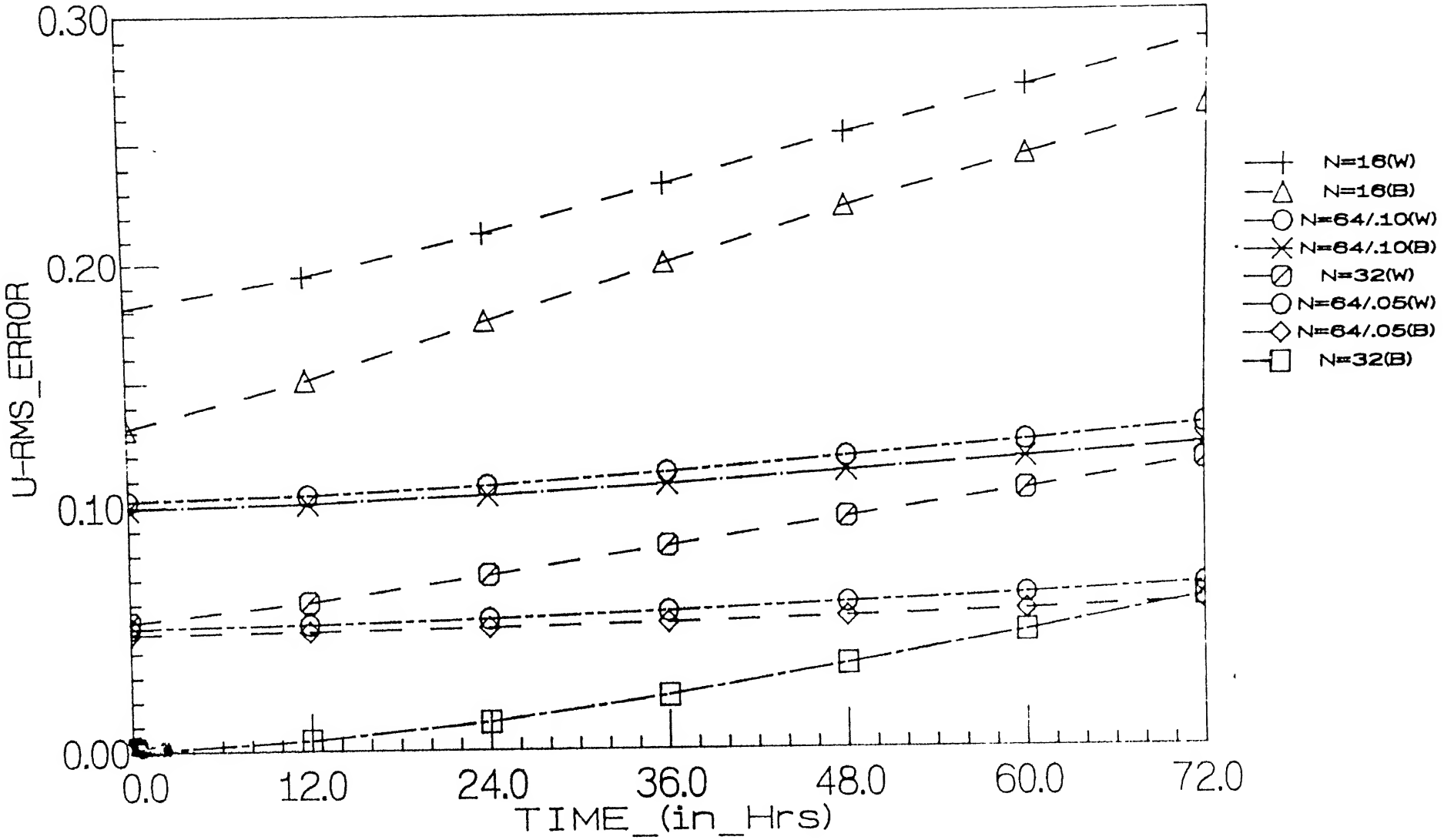

FIG.(3a)_RESOLUTION_vs_IC_ERROR(U-VEL)

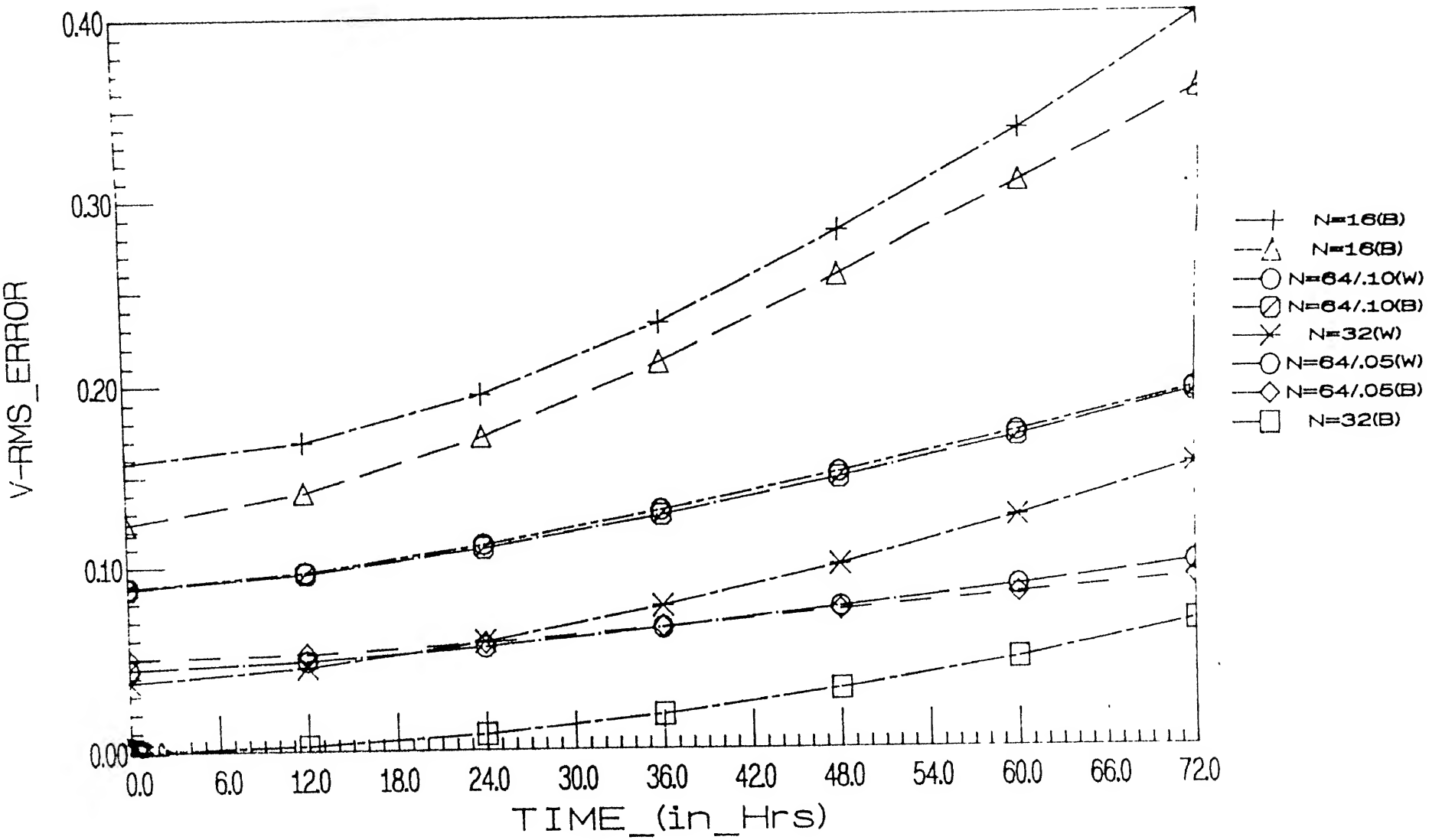

FIG.(3b) RESOLUTION_vs_IC_ERROR(V_VEL)

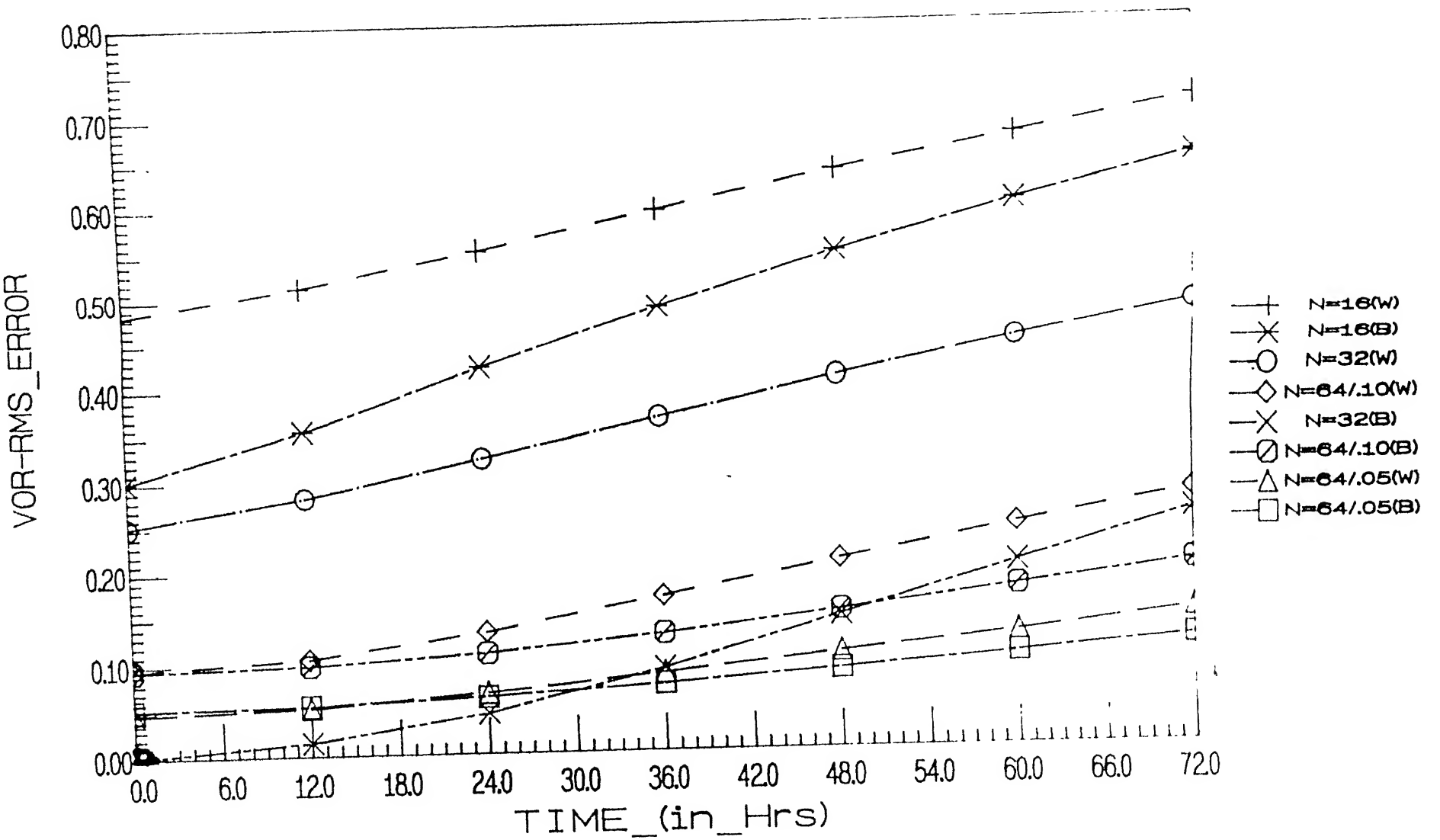

FIG.(3c) RESOLUTION_vs_IC_ERROR(VORTICITY)

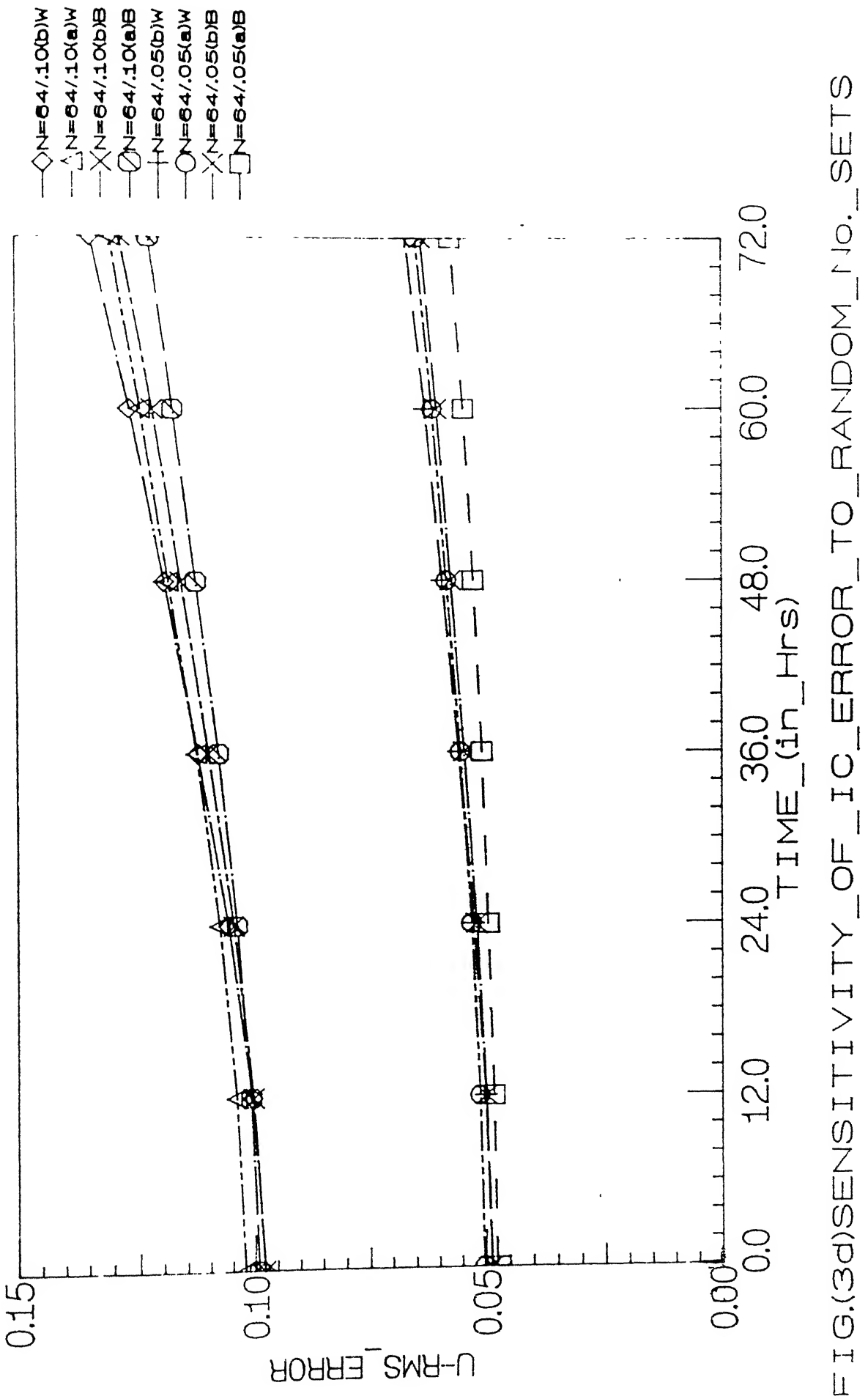

FIG.(3d)SENSITIVITY_OF_IC_ERROR_TO_RANDOM_No._SETS

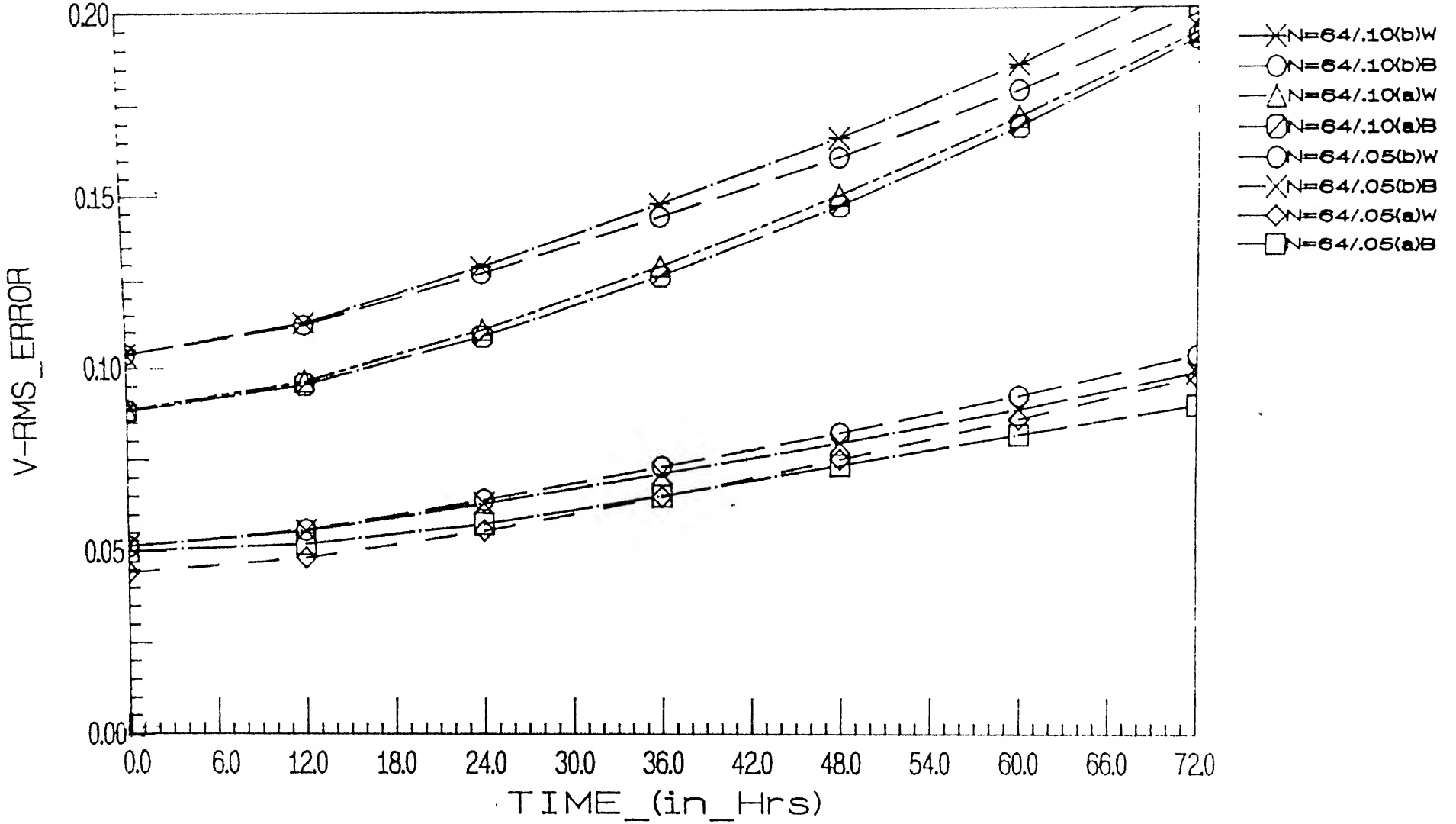

FIG.(3e)SENSITIVITY_OF _IC_ERROR_TO_RANDOM_No._SETS

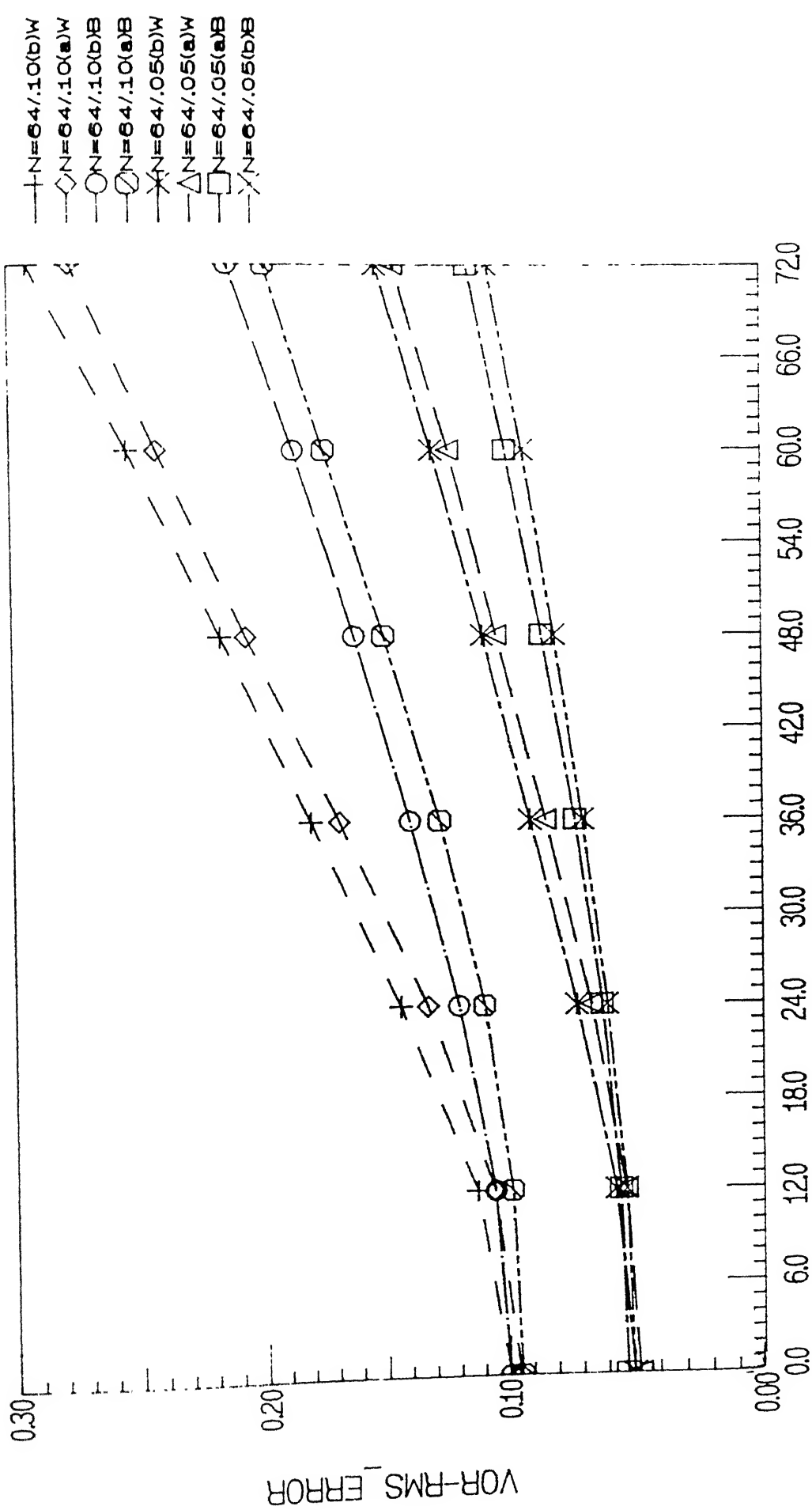

FIG.(3f)SENSITIVITY_OF_IC_ERROR_TO_RANDOM_No._SETS

coefficients as those that corresponds to a truncation number of N=16. This includes the first 256 coefficients. 'High wave number' coefficients are those that fall outside this region. In both cases we do two simulations each corresponding to rms error of approximately 5% on velocity fields.

To introduce error in the high wave number or on the low wave number coefficients, we use pseudo random numbers of uniform distribution with zero mean and specified standard deviation. We have to calculate the standard deviation for the high wave number error (σ_H) case as well as for the low wave number error (σ_L) case which will give the specified SD (standard deviation) of 0.05 for the total field. The expression for calculating new SD is given as

$$\frac{\sigma_H^2 E_H}{E} = \sigma^2 \qquad \text{and} \qquad \frac{\sigma_L^2 E_L}{E} = \sigma^2 \tag{4.5.1}$$

where E_H and E_L are the energy contained in the high and low wave numbers, respectively. E is the total energy in the initial condition (includes high wave number as well as low wave number coefficients), σ is the standard deviation of the whole field (0.05) which we want to specify, and σ_H and σ_L are the SD for the error introduced in the high wave number coefficients and the low wave number coefficients respectively. The error is introduced on the desired coefficients using equation (4.4.1). In this way we generate our new set of initial conditions.

Again the computations are performed on the 192×160 grid for the 3-days. The rms error is computed using (4.3.3).

Fig(4a) and Fig(4b) present plots of RMS error in U and V,respectively, vs time for the low wave number (Lo) and the High wave number (Hi) cases. To also get an idea of the variation

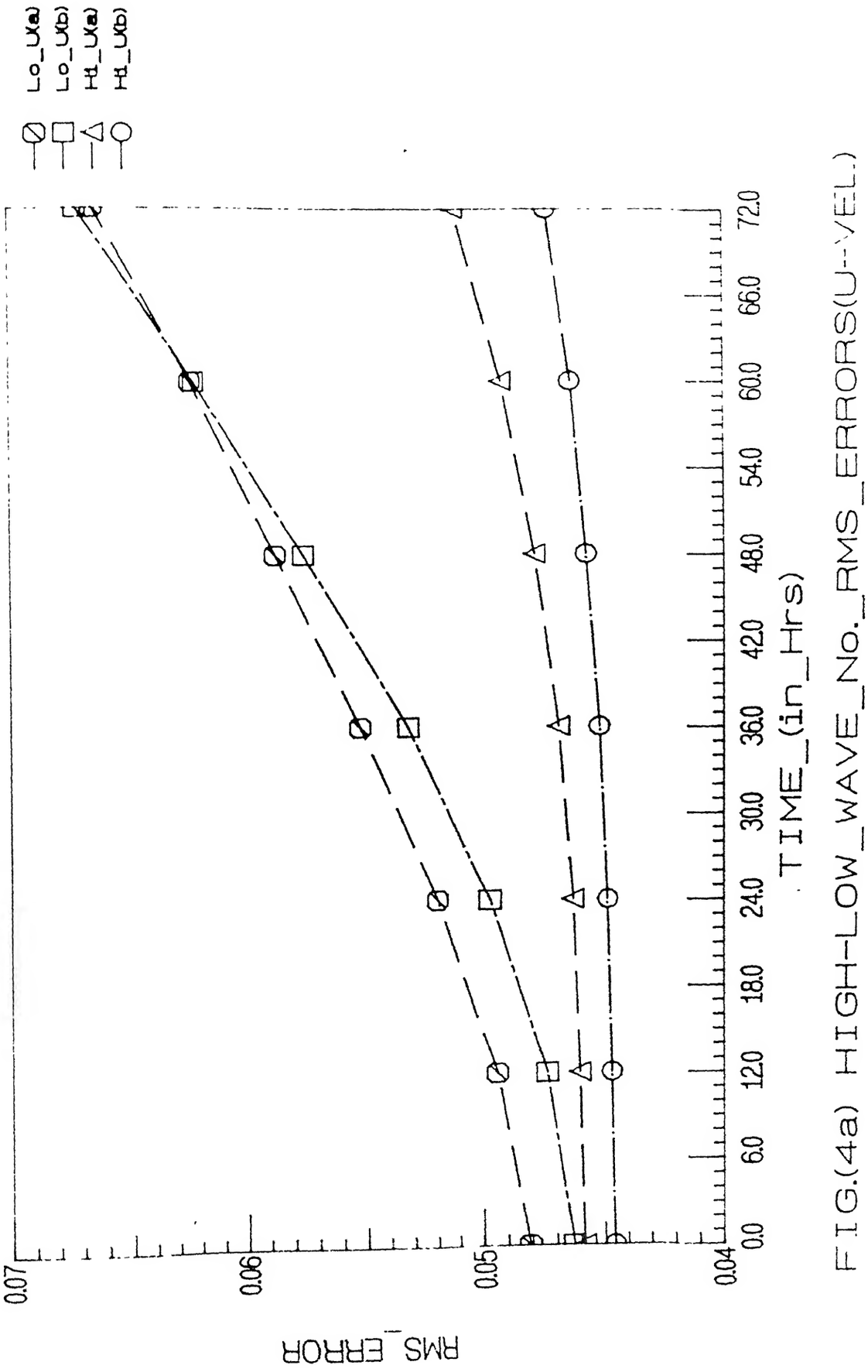

FIG.(4a) HIGH-LOW_WAVE_No._RMS_ERRORS(U-VEL.)

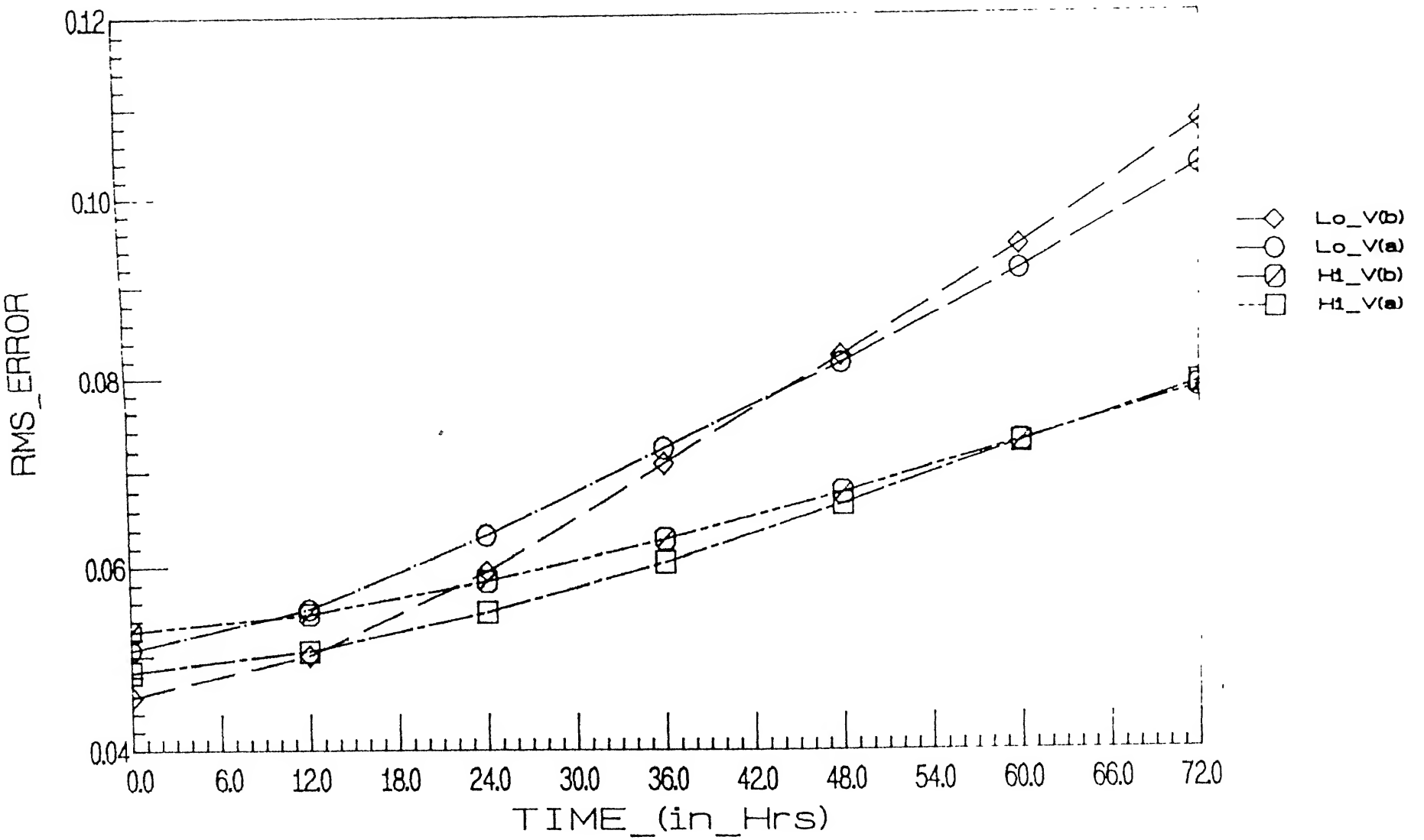

FIG.(4b) HIGH-LOW_WAVE_No._RMS_ERRORS(V-VEL)

caused by different random number sequence (used in introducing the initial error), two different runs were performed for each case with with two different random number sequences (a) and (b). It can be seen from the figures that the initial error is in each case is not exactly 0.05. This is because error is introduced in the vorticity field (as we are using the vorticity equation) and the error in the U, V fields cannot be precisely determined *a priori*. However the initial errors are close enough for the purpose of qualitative comparison.

It can be seen from the Fig(4a) and Fig(4b) that for the low wave number case the RMS error for both U and V fields increases much more rapidly than in the high wave number case. Therefore it can be concluded that, for approximately the same amount of total initial RMS error, the predictions are much more sensitive to the small wave number (large-scale) coefficients than the large-wave number (small-scale) coefficients.

It can also be observed from the figures that the curves for the two different sets of random number (a) and (b) are qualitatively similar. Therefore, the above stated conclusions are independent of the random error introduced.

CONCLUSIONS AND SCOPE FOR FURTHER WORK :

The present work has shown that the truncation number N=32 is an optimum resolution, if our IC contains 5-10% RMS error, for 3-day prediction of the velocity field. However, the vorticity field requires higher resolution. It is also found that the predictions are much more sensitive to errors in the lower order coefficients than in the higher order ones. The error introduced by truncation of IC is found to have slow growth rate if sufficiently high resolution is used.

The random number dependence test has also been carried out in our study. We observed that the results are qualitatively similar and are, thus, independent of the random number sets used to introduce error on IC.

A very interesting extension to the present work would be the study of error spectra, the distribution and growth of error in the wave number space. During the course of the present work, this study has been investigated to a limited extent. It would also be interesting to do similar resolution v/s ICD error comparison using more realistic models.

BIBLIOGRAPHY

1. Thompson, P.D., 1957: *Uncertainty of initial state as a factor in the predictability of large scale atmospheric flow patterns.* Tellus, 9, 275-295.

2. Loenz, E.N., 1969: *The predictability of a flow which possesses many scales of motion*, Tellus, 17, 321-333.

3. Kraichnan, R.H., 1970: *Instability in fully developed turbulence*, Phys. Fluids, 13, 569-575.

4. Leith, C.E., 1971: *Atmospheric predictability and two dimensional turbulence*, J. Atmos. Sci., 28, 145-161.

5. Leith, C.E., and R. H. Kraichnan, 1972: *Predictability of the turbulent flows*, J. Atmos. Sci., 29, 1041-1058.

6. Basdevant, C., B. Legras, R. Sadourny and M. Beland 1981: *A study of the Barotropic model flows: Intermittancy, waves and predictability*, Atmos. Sci., 38, 2305-2326.

7. Holloway, G., 1983: *Effects of the planetary wave propagation and finite depth in the predictability of atmospheres.* J. Atmos. Sci., 39, 314-327.

8. Vallis, G.K., 1983: *On the predictability of quasi-geostrophic flow: The effect of beta and baroclinicity*, J. Atmos. Sci., 40, 10-27.

9. Roads, J.O., 1985: *Temporal variations in predictability*, J. Atmos. Sci., 42, 884-903.

10. Strauss, D.M., 1989: *Baroclinic instability and wave-wave interactions in quasi-geostrophic error growth*, J. Atmos. Sci.,

42, 2380-2403.

11. Charney, J.G., R.G. Fleagle, V.E. Lalley, H. Riehl and D.Q. Wark, 1966: *The feasibility of a global observational and and analysis experiment*, Bull. Amer. Meteor. Soc., 47, 200-220.

12. Smagorinsky, J.,1969: *Problems and promises of deterministic extended range forecasting*. Bull. Amer. Soc., 50, 286-311.

13. Williamson, D.L., and A. Kasahara. 1971: *Adoption of meteorological variables forced by updating*. J. Atmos. Sci.. 28, 1313-1324.

14. Baede, P., D. Dent and A. Hollingworth, 1977: *The effect of metric precision on some meteorological integration*,

15. Orszag, S.A., 1970: *Transform method for the calculation of vector-coupled sums: application to the spectral form of the vorticity equation*, J. Atmos. Sci., 27, 890-895.

16. Haltiner, G.J., and R. J. Williams, 1980: *Numerical Prediction and Dynamic Meteorology*, John Wiley and Sons, New York.

17. Holton, J.R., 1979: *An Introduction to Dynamic Meteorology*, *Academic Press*, New York.

18. Washington, W.M., and C.L. Parkinson, 1986: *An Introduction to Three-Dimensional Climate modeling*, *University Science Books*, Oxford University Press.